UNIVERSITY
OF SUSSEX

5G Mobile Communications and Intelligent Embedded Systems

864H1: MSc Individual Project

Dissertation

Beamforming with Software-Defined Radio

Advisor: Falah H. Ali

Candidate Number: 268272

Word count: 13396

Abstract

This dissertation elucidates the intricacies of creating and analyzing practical digital wireless communication systems, with a keen focus on integrating digital beamforming using two bladeRF SDR devices. Chapter 1 offers a clear roadmap, defining both the project's description and overarching objectives. Chapter 2 serves as a bedrock, presenting requisite background knowledge pivotal for comprehending the methodologies tailored to meet the project's aims. In Chapter 3, the project dives into the mechanics of achieving digital communication. Utilizing MATLAB/Simulink, the author crafts a practical wireless communication framework while addressing inherent challenges. A hallmark of this chapter is the author's development of a novel MIMO block, specifically designed to facilitate MIMO communication with bladeRF. This innovation is anticipated to enrich the community's toolbox. Chapter 4 is an empirical exploration. Various wireless systems, namely SISO QPSK, 1x2 Receive diversity with EGC, and both 1x2 Receiver and 2x1 Transmitter beamforming, are rigorously tested, contrasted, and analyzed. An ADALM-Pluto SDR device introduces interference, permitting an investigation into the BER dynamics of these systems under external disruptions. The findings and their implications are subsequently discussed in-depth, offering a holistic understanding of the field's challenges and the solutions posited in this work.

Acknowledgements

I wish to express my profound gratitude to the University of Sussex for affording me the invaluable opportunity to further my academic pursuits within its esteemed walls. My deepest appreciation extends to the dedicated staff of the 5G Mobile Communications and Intelligent Embedded Systems program. In particular, Prof. Falah H. Ali deserves special mention for his unwavering guidance and support throughout this journey; his insights and mentorship were instrumental in realizing this work. Lastly, I cannot conclude without acknowledging the bedrock of my support system - my family. To them, and especially to my mother, Filiz Duman, I owe a debt of gratitude that words can scarcely capture. Her unwavering belief in my capabilities and her ceaseless encouragement have been the twin pillars upon which I've built my academic edifice.

Statement of Originality

This document constitutes the summation of my individual research endeavor for the Master of Science degree at the University of Sussex. The Modulator and Receiver architectures presented in the Simulink subsystem, as expounded upon in section 3.4.1, are predicated upon exemplars provided by Mathworks, with appropriate citations furnished therein. Additionally, the antenna mounting apparatus delineated in figure 31, referenced in section 3.6, was the scholarly work of my colleague, Mr. Yunus Yunal. I, Muhammed Emre DUMAN, certify that the attached dissertation is my own original work except where otherwise indicated. I have referenced my sources of information; in particular I have placed quotation marks before and after any passages that have been quoted word-for-word and identified their origins.

Muhammed Emre DUMAN

Signed: 

Date: 23.08.2023

Table of Contents

Chapter 1 : Introduction

1.1. Project Description

In recent years, the dynamic realm of digital beamforming has garnered significant attention, especially when applied through the versatility of Software-Defined Radio (SDR) devices. This thesis delves deeply into this intersection of technology, with a primary objective of establishing a robust digital communication pathway between two distinct SDR devices, and subsequently enhancing this link using a meticulously chosen beamforming technique. At the onset, the report embarks on an expansive literature review, intended to offer readers a holistic understanding of three pivotal areas: the multifaceted nuances of digital communication, the foundational and advanced concepts of beamforming, and the ever-evolving world of software-defined radio technology.

With the background firmly established, the narrative then transitions to the heart of the research: the methodology. Here, readers are taken on a journey through the simulation process. The digital communication system, now conceptually intertwined with the selected beamforming algorithm, is presented in a simulated environment, providing a theoretical blueprint for subsequent practical applications.

The ensuing sections dive into the specifics of the SDR device selection process. Not all SDR devices are created equal, and the report sheds light on the criteria, considerations, and ultimate rationale behind the chosen devices. This is followed by a detailed exploration of the interface dynamics, particularly focusing on the symbiotic relationship between the physical hardware components and the MATLAB/Simulink environment. Such integration is crucial, not only for seamless data flow but also for accurate and real-time computations essential for beamforming.

One cannot overstate the importance of antenna mounting in any beamforming project. Hence, an entire section is dedicated to discussing various strategies, challenges, and solutions in the realm of antenna placements and orientations. This ensures optimal reception and transmission of signals, further enhancing the efficacy of the beamforming techniques applied.

The penultimate phase of the report captures the culmination of the research: the real-world implementation. Here, the theoretical constructs and simulated models are brought to life, with each step of the implementation narrated in detail. The final challenges, tweaks, and triumphs are all laid bare.

Lastly, the thesis reaches its zenith in the test and validation segment. This section doesn't just serve as a recapitulation. Instead, it critically assesses and juxtaposes findings from both the simulated scenarios and real-world trials, offering insights, drawing conclusions, and perhaps even laying the groundwork for future endeavours in this exciting field.

1.2. Objectives

The primary objective of this thesis is to explore and understand the potential of digital beamforming when facilitated through Software-Defined Radio (SDR) devices. Within this overarching goal, the project seeks to achieve the following specific aims:

1. **Establishment of Digital Communication**: To successfully create practically a reliable and efficient digital communication link between two SDR devices. This forms the fundamental groundwork upon which further enhancements via beamforming techniques will be built.
2. **Application of Beamforming:** To harness the principles and techniques of digital beamforming, integrating it with the previously established SDR communication link. This step aims to augment the strength, reliability, and directionality of the signal communication between the devices.
3. **Analysis and Optimization:** Once the beamforming technique is applied, the objective extends to analysing its impact on the digital communication link, identifying areas of improvements, and subsequently optimizing the process for enhanced performance.

Through these objectives, the thesis hopes to contribute meaningful insights and developments to the field of digital communication, particularly highlighting the symbiotic potential between beamforming and SDR technology.

Chapter 2 : Background

2.1. Digital Communication

2.1.1. Introduction

In this MSc project, QPSK transmitter and receiver are used to create communication between two SDR devices. Therefore, implementation of a practical QPSK transmitter and receiver is going to be investigated in this section of the report such as carrier frequency and phase offset, timing drift and frame synchronization. Before going into details of QPSK transmitter and receiver, basics of wireless digital communication is going to be explained. The overall view of wireless digital communication can be briefly explained as follows: wireless digital communication refers to the transfer of information using electromagnetic waves, such as radio waves, microwaves, and infrared, in the absence of physical connections like wires [1] [2]. This method involves encoding information as binary data (comprising 0s and 1s), which has the advantage of being less susceptible to interference [2]. The digital data can be then modulated onto carrier waves through techniques like QAM, PSK, and FSK, making it suitable for transmission. The choice of modulation technique depends on various factors such as the desired data rate, bandwidth efficiency, and the characteristics of the communication channel. For example, PSK modulation is commonly used in optical transmission systems due to its resistance to nonlinear effects present in the optical transmission medium and multi-level PSK variations, such as QPSK and 8PSK, are advantageous as they represent multiple bits with a single-phase shift [3]. Common devices leveraging this form of communication range from mobile phones and Wi-Fi routers to more complex systems like satellites [4]. To ensure universal compatibility and efficient data exchange, several standards, and protocols, including Wi-Fi (IEEE 802.11), Bluetooth, and 5G have been established [5]. The main allure of wireless digital communication lies in its mobility and flexibility, allowing users to remain connected without being tethered and facilitating communication in areas where traditional wired setups are impractical [6]. However, this freedom also introduces challenges, such as potential interference from other devices, and security concerns [6] [7] [8]. Regardless of these challenges, the convenience and adaptability of wireless communication may have made it an indispensable tool, impacting everything from personal communications like mobile phones to large-scale networks in satellite communication and sensor networks.

2.1.2. Elements of Wireless Digital Communication

Digital communications focus on sending data in a digital format from its originating point to one or multiple endpoints. When analysing and designing such communication systems, the properties of the physical channels transmitting the information are crucial [2].

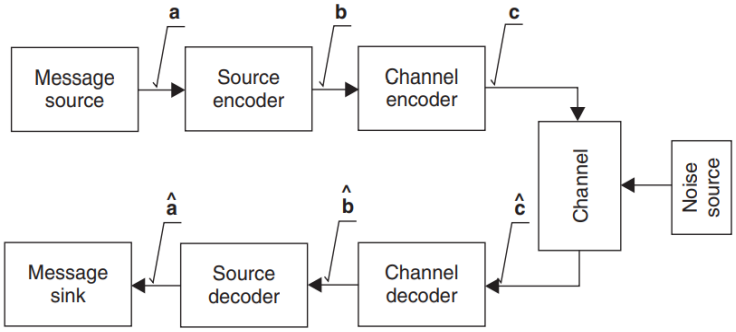

Figure 1 - Basic model of a discrete communication system [9]

The functional diagram and essential components of a digital communication system are shown in Figure 1. The output of "Message source" in Figure 1 can be an analogue signal like audio or video signal, or a digital signal that can be produced by a computer. The produced output from message source should be converted into binary digits sequence. The efficient conversion of the message is called source encoding or data compression and it is represented in Figure 1 as "Source encoder" [2] [9]. The output of the source encoder can be passed to "Channel encoder" in Figure 1 in order to ensures reliable data transmission between the source and receiver by adding controlled redundancy to the information sequence. This added redundancy counters the effects of noise and interference during transmission [2] [9] [10].

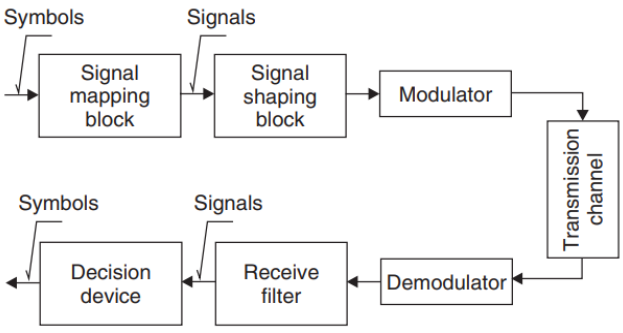

Figure 2 - Example of internal structure channel block [9]

In a communication system, the channel operates autonomously from other system components. From an information theory perspective, a channel is seen as a sequential linkage of several physical units, the

composition and arrangement of which are determined by the design of the particular system in question. In this context, the channel component might take on roles such as converting the symbols from the channel encoder into data symbols, the responsible block is “Signal mapping block” in Figure 2. On the other hand, “Signal shaping block” in Figure 2 is responsible for shaping the waveform of these data symbols to fit the channel's bandwidth and modulating the signal to align with the frequency range of the physical channel [9]. Transmission channel in Figure 2 refers to the physical means for sending the signal by the transmitter to the receiver. In wireless communication, the channel is subject to the impairments include:

1. Channel distortion that can manifest as multipath interference, where numerous replicas of the same signal interfere with each other, either amplifying (constructive) or weakening (destructive) the received signal.

2. Time-varying nature, resulting from either the movement of the terminal or alterations in the conditions of the transmission route.

3. Interference occurs when other sources, either accidentally or deliberately, produce output signals that share the same frequency range as the transmitted signal.

4. Receiver noise is generated by electronic components at the beginning of the receiver. Even though it originates at the receiver, this noise is commonly viewed as an effect of the channel, hence it's sometimes called channel noise. The impact of this receiver noise varies based on the strength of the received signal. Notably, this signal strength is greatly influenced by the transmission path between the transmitter and the receiver [11].

On the receiving end, the channel block may include components like an amplifier, a demodulator, a reception filter, and a decision-making device that produces estimations of the signals that the channel decoder can accept. These estimations can occasionally be enhanced with extra information that informs subsequent receiver components about the trustworthiness of the provided symbols [9].

2.1.3. End-to-End Communication

In this part of the report, how the elements used in wireless communication explained in section 2.1.2 can be implemented to create practical end-to-end communication will be explained together with the alternatives. The illustration of physical layer of wireless communication is shown in Figure 3. The physical layer of wireless communication acts like a communication pipe between the information's origin and its destination [11].

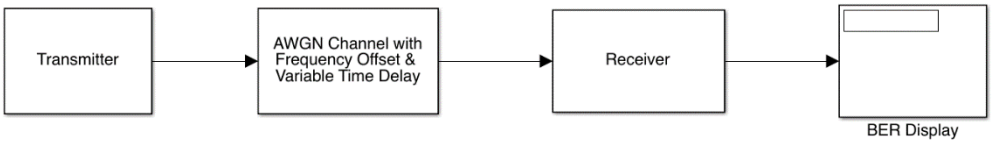

Figure 3 - Illustration of physical layer of wireless communication

2.1.3.1. Transmitter Side

Therefore, the transmitter side in Figure 3 can contain "Message Source", "Source Encoder", "Channel Encoder" which may consist of "Signal mapping block", "Signal Shaping block" and "Modulator".

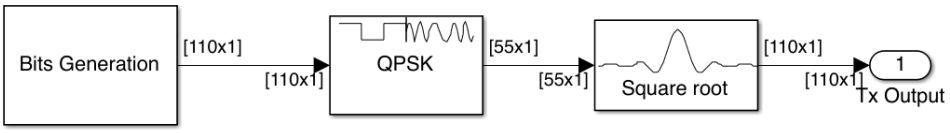

Figure 4 - Illustration of transmitter side

Figure 4 shows the example of transmitter architecture which is also used in the project to implement transmitter side. The role of "Bits Generation" block is "Message Source" and "Source Encoder" which are explained as converting the information into binary sequence in section 2.1.2. "QPSK" block can be considered as "Signal Mapping block" and "Modulator" where "Square root" block can be "Signal Shaping block" because Quadrature Phase Shift Keying (QPSK) is a prominent digital modulation scheme employed in Phase Shift Keying modulation scheme characterized by its dual functionalities of signal mapping and phase modulation to convey binary information [12] [13]. On the other hand, there are alternative digital modulations schemes such as Amplitude Shift Keying (A.S.K) and Frequency Shift Keying (F.S.K.). To explain the reason for choosing the PSK technique, the comparison of other techniques is as follows: Amplitude Shift Keying (ASK) stands out for its simplicity and power efficiency. However, this technique is highly vulnerable to noise and interference due to its reliance on amplitude variations, making it less robust in fading environments [12]. On

the other hand, Frequency Shift Keying (FSK) offers more robustness against amplitude distortions, given that it encodes data through frequency changes. Despite its greater resilience in noisy conditions compared to ASK, FSK demands more bandwidth and introduces a higher level of complexity in demodulation [12]. Phase Shift Keying (PSK), specially forms like BPSK and QPSK, provides bandwidth efficiency. It proves to be more robust against additive white Gaussian noise, and its ability to send multiple bits per symbol, as in QPSK, enhances data rate efficiency [14]. Yet, PSK is not without its challenges, including sensitivity to phase noise, jitter, and the need for sophisticated synchronization. In order to compensate for these problem, “Square root” block is introduced to achieve better performances in terms of minimizing Inter-Symbol Interference (ISI), controlling bandwidth, and Smooth transition [12]. It is also known as Root Raised Cosine filter, and it can be considered as “Signal Shaping block”.

2.1.3.2. Wireless Channel

After these blocks, the signal can be transmitted through the wireless channel. However, the transmitted signal is subjected to channel impairments that refer to the various factors that degrade or distort the transmitted signal as it travels from the transmitter to the receiver. Some of the common channel impairments in wireless communication include:

Path Loss: As a wireless signal travels, it attenuates (or loses strength). The signal strength decreases as a function of the distance between the transmitter and the receiver [15].

Shadowing: As the signal passes through obstacles (like buildings, trees, hills, etc.), it can be blocked or attenuated. This can cause areas where the signal strength is significantly lower than surrounding areas, creating "shadows" [15].

Multipath Fading: In urban or cluttered environments, a signal can bounce off multiple surfaces (like buildings, vehicles, etc.) before it reaches the receiver. This results in multiple copies of the same signal arriving at the receiver at slightly different times, leading to constructive and destructive interference patterns. This can cause rapid fluctuations in the signal's amplitude and phase [15].

Doppler Shift: When there's relative motion between the transmitter, the medium, and the receiver, the frequency of the received signal can differ from the transmitted frequency due to the Doppler effect. This shift in frequency can cause problems, especially for narrowband systems [15].

Interference: Other transmitting devices or sources of electromagnetic energy can interfere with the intended signal. There are several types of interference, including co-channel interference (from devices using the same frequency) and adjacent-channel interference (from devices using nearby frequencies) [15].

Noise: All electronic devices produce some level of noise. In wireless communication, the receiver picks up this noise along with the desired signal. The most common type of noise is thermal noise, which is caused by the random motion of electrons in conductors [15].

Therefore, "AWGN channel with frequency off set and variable time delay" block in Figure 4 represents some of the channel impairments such as multipath fading, doppler shift and noise. Due to the introduced channel impairments and PSK communication is sensitive to the phase noise and jitter, the receiver side complexity may increase in practical manner. Hence, to cope with these challenges, the receiver side may need to have solution for frame detection, timing recovery, carrier recovery channel state information estimation [16].

2.1.3.3. Receiver Side

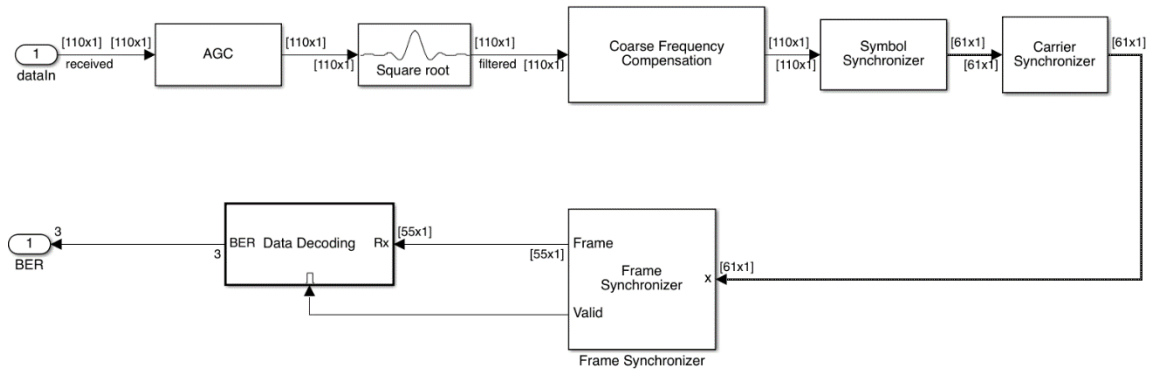

Figure 5 - Practical example structure of receiver side

Figure 5 shows a practical receiver side structure that can handle the mentioned challenges in wireless channel. First block is AGC (Automatic gain controller) that adjusts the gain in the reception chain adaptively. When confronted with overly strong signals, it decreases the gain to prevent saturation, and inversely, when signals are faint or weakened, it compensates by increasing the gain. This adaptive behaviour ensures that the received

signal strength remains within an optimal range, facilitating consistent and high-quality data reception. The primary objective of the AGC system is not only to maintain the signal within a range that prevents clipping distortion in Analog-to-Digital Converters (ADCs) but also to ensure that downstream components, like demodulators and decoders, can operate efficiently and without error [17]. After AGC, the Raised Cosine Receive Filter can be used to provide matched filtering for the transmitted waveform. Then, the synchronization blocks can be introduced to solve carrier frequency and phase offset, timing drift and frame synchronization issues in wireless communication.

2.1.3.4. Synchronization at Receiver Side

Synchronization is a pivotal process that ensures the precise timing and alignment of received signals for accurate data interpretation. One vital aspect, carrier synchronization, is indispensable for coherent PSK schemes, as it aligns the phase of the received signal with the local oscillator [18]. Moreover, the oscillator at the transmitter and receiver don't have the exact same frequency. This means when the transmitter sends a signal, and the receiver processes it, they aren't perfectly aligned. This mismatch causes the received signal's pattern (or constellation) to appear as if it's rotating [19].

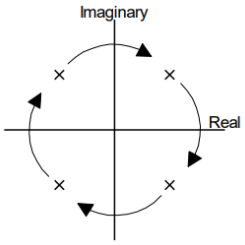

Figure 6 - Rotation of Constellation Due to Carrier Offset [19]

Other vital aspect, symbol synchronization, universally required across digital modulation schemes, guarantees accurate sampling of received symbols [18]. Furthermore, data in wireless systems is typically transmitted in structured frames. Recognizing the start of these frames is paramount for decoding; however, challenges arise due to factors like propagation and signal processing delays which can obscure the exact commencement of a frame. Consequently, frame detection becomes an essential facet of a communications receiver, solidifying its role in the broader domain of receiver synchronization [16].

2.2. Beamforming

2.2.1. Introduction

Beamforming is a method used to direct signals in specific directions when transmitting or receiving. Essentially, it's a form of spatial filtering, where signals are processed to be sent or received more effectively using an array of sensors or antennas. By adjusting the angles of these sensors, the signals can be strengthened or weakened, allowing for more focused communication [20]. This technique is applied at both the transmission and reception stages to ensure precise signal transmission and reception. Beamforming isn't just limited to wireless communication; it's also used in various fields like sonar, radar, seismology, acoustics, radio astronomy, and biomedicine [21]. Adaptive beamforming, in particular, fine-tunes the received signal by rejecting unwanted interference and focusing on the desired information. The specific approach to beamforming can vary based on the arrangement and combination of antennas used [22].

2.2.2. Advantages of Beamforming

Beamforming offers advantages including enhanced spectral efficiency, improved energy efficiency, suitability for mmWave bands, and bolstered system security [22].

2.2.2.1. Enhanced Spectral Efficiency

The integration of beamforming antenna elements facilitates capacity augmentation through the deployment of training sequences, enhancement in signal fidelity, and power regulation for both uplink and downlink transmissions. When base stations (BSs) are equipped with extensive antenna arrays designed for beamforming, accompanied by coherent precoding, and refined detector processing, there's a consequent potential for massive MIMO systems to bolster the spectral efficiency (SE) of a wireless communication framework. It's worth noting that the spectral efficiency of cellular systems at mobile terminals is predominantly influenced by the distribution of the carrier-to-interference ratio [23].

2.2.2.2. Improved Energy Efficiency

The energy requisite for transmitting signals to a designated user via beamforming antennas is notably minimal. One method to diminish power expenditure involves ascertaining the optimal, precise count of elements that align with the predefined criteria essential for managing an expansive MIMO system. A judicious execution of

this methodology can culminate in a system characterized by reduced amplifier expenses and diminished power consumption. The average efficiency, as observed from utilizing multiple base stations (BSs), appears to be agnostic to the quantity of antennas encompassed within a singular cell. Consequently, a plausible approach entails employing a uniform set of antennas across all constituent cells of the system. Furthermore, power regulation can serve a dual purpose: curtailing power usage and concurrently adhering to the throughput prerequisites of a given terminal [23].

2.2.2.3. Suitability for mmWave bands

Given that the majority of frequency bands designated for wireless cellular communication are licensed, leveraging segments proximate to the mmWave spectrum can enhance achievable data rates. Specifically, frequencies of 60 GHz and beyond offer considerable promise. One salient advantage of such frequency ranges is their expansive bandwidth. Yet, they often exhibit challenges in short-distance signal transmission, which can be mitigated through the employment of highly directive antennas. The presence of high-frequency carrier components enables the utilization of compact antennas with significant gains, particularly beneficial for mobile devices. Additionally, while narrow and fixed beams may not be directly compatible with mobile devices, this can be addressed effectively through beamforming techniques [23].

2.2.2.4. Enhanced System Security

Beamforming aims to direct a transmitted signal precisely to its intended receiver while ensuring protection from potential malicious entities. Relative to traditional antennas, beamforming exhibits a reduced susceptibility to eavesdropping, thereby enhancing physical security [23].

2.2.3. Classification of Beamforming

2.2.3.1. Analog beamforming

Analog beamforming is a way to control the direction of a signal. It uses devices called low-phase shifters and hybrid matrices. This method changes the signal using analogue tools. When trying to save money, people choose analogue beamforming because they can use cheaper parts, like low-cost phase shifters, instead of digital methods [24].

2.2.3.2. Digital beamforming

Digital beamforming is a way to adjust both the direction and strength of a signal using tools like RF chains and a baseband. People often choose digital beamforming when they want a strong signal but don't want too much outside interference. This method comes in two main types. The first is "fixed," where the settings stay the same all the time. The second is "adaptive," which changes its settings based on the surrounding conditions, often making it more effective. These two main types can be split further into four groups: one fixed direction for one user, one fixed direction for many users, one changing direction for one user, and one specific changing direction for multiple users [24].

2.2.3.3. Hybrid beamforming

Hybrid beamforming is a technique used in wireless communication systems, especially in scenarios like 5G networks, to exploit the benefits of both analogue and digital beamforming while mitigating their respective drawbacks. This combines both methods. Typically, a subset of antennas is grouped together and controlled using analogue beamforming, while digital beamforming is used to manage the signals across these groups. This approach attempts to strike a balance, offering a level of flexibility and performance that's more resource-efficient and cost-effective than pure digital beamforming [25].

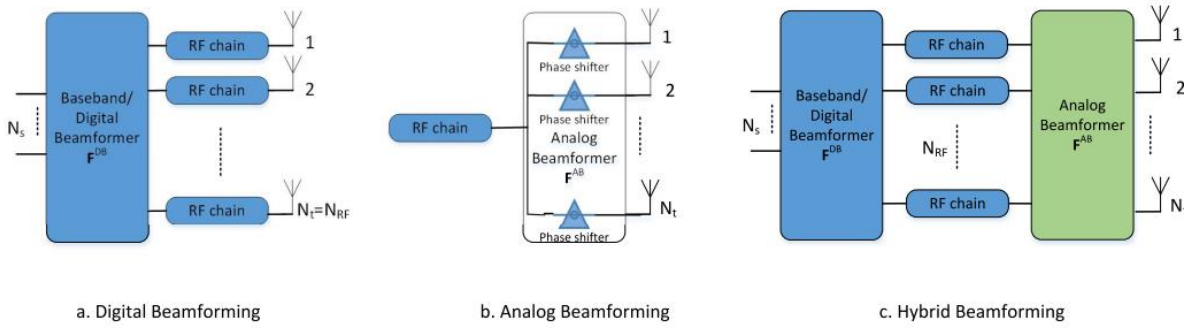

Figure 7 - Beamforming architectures [41]

2.3. Software-Defined Radio

2.3.1. Introduction

Software Defined Radio (SDR) represents a paradigm shift in the realm of radio communication, transitioning away from traditional hardware-centric approaches to more software-centric methodologies. At its core, SDR allows for a significant portion of signal processing, which was traditionally accomplished via hardware (like

mixers, filters, amplifiers), to be executed in software. This confers unparalleled flexibility, enabling a single piece of hardware to operate across multiple frequencies and modulation schemes purely by altering the software [26]. The emergence of SDR holds the promise of revolutionizing wireless communication, facilitating more adaptive and versatile radio systems capable of meeting the ever-evolving demands of modern communication networks.

2.3.2. Architecture

In this part, the overarching architecture of Software Defined Radios (SDRs) is going to be investigated and elucidated their primary components and associated processing prerequisites. As highlighted in the previous section, SDRs are instrumental in the evolution of wireless standards, attributed largely to their inherent flexibility and straightforward programmability. This can be traced back to the digital signal processing and digital front-end operations—encompassing channel selection, modulation, and demodulation—predominantly occurring within the digital realm. Typically, these operations are executed via software on computational platforms like General Purpose Processors (GPPs) and Digital Signal Processors (DSPs). Nonetheless, these tasks can also be dispatched on reconfigurable hardware platforms, notably Field-Programmable Gate Arrays (FPGAs) [27].

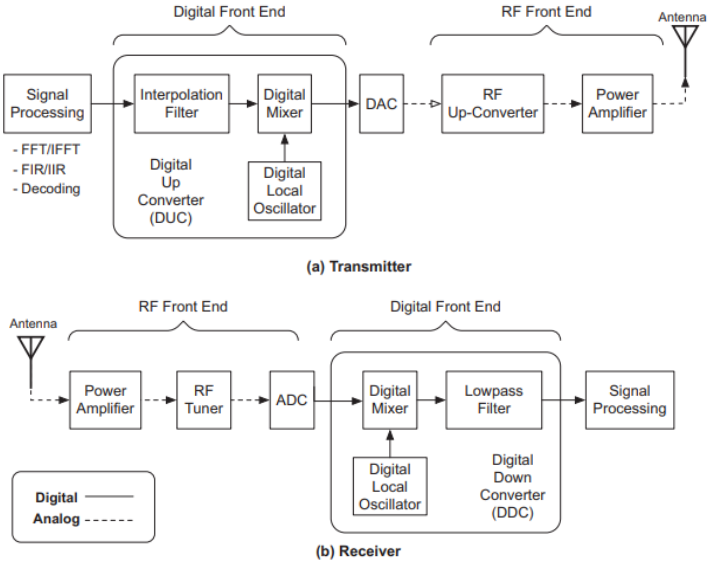

Figure 8 – Transmitter and Receiver architecture of SDR [27]

Figure 8 shows a typical Software-Defined Radio transceiver includes: Signal processing, Digital Front End, RF Front End (Analog), and antenna. From the perspective of the transmitter, the process initiates with the

generation of a baseband waveform, succeeded by the creation of an Intermediate Frequency (IF) waveform. Subsequently, a Radio Frequency (RF) waveform is synthesized and propagated through the antenna. On the receiver's end, the RF signal undergoes sampling, demodulation, and decoding. Delving deeper into the reception mechanism: The RF signal procured from the antenna is augmented via a specifically tuned RF stage, amplifying a designated frequency bandwidth. This intensified RF signal transitions to an analogue IF signal, which the Analog-to-Digital Converter (ADC) then transfigures into digital samples. This data stream is relayed to a mixer stage. The mixer, an intricate electrical configuration designed to intake dual signals and produce a novel frequency, concurrently receives input from a local oscillator, its frequency dictated by the tuning apparatus. Consequently, the mixer repositions the incoming signal to baseband. Following this, the signal encounters a Finite Impulse Response (FIR) filter, which is essentially an amalgamation of multiply-add units and shift registers. This filter specifically restricts the signal bandwidth, functioning as a decimating low-pass filter. The digital downconverter is replete with a multitude of multipliers, adders, and shift-registers to facilitate the previously mentioned operations. The ensuing signal processing phase encompasses procedures like demodulation and decoding. Typically, this intricate phase is managed by specialized hardware such as an Application Specific Integrated Circuit (ASIC) or adaptable alternatives like FPGA or DSP [27].

2.4. Underlying Mathematics

2.4.1. Constellation and Bit mapping (Digital Modulation)

Symbol mapping pertains to the assignment of data bits to specific symbols within the digital domain. For the variants of symbol mapping addressed in this text, symbols can be delineated as a series of complex numerals, denoted as d_n which can take a finite set of possible values. The value of d_n is based on the bits it stands for. So, for each d_n value, there's a clear link to a set of bits, like $\{b_1, b_2, \dots, b_k\}$ Here, K is how many bits one symbol can show. The way this works is based on the type of modulation used [10]. The rate at which new symbols are sent is referred to as the symbol or signalling rate, represented as R . Frequently, the data rate is symbolized by R_b in bits per second. Therefore, the symbol rate and symbol period can be written as [15]:

$$R_b = kR \ \ and \ \ T_s = \frac{1}{R_b} \qquad (2.4.1) \quad [15]$$

A modulation is termed "M-ary" when its alphabet encompasses M potential values. Consequently,

$$K = log_2 M \text{ , where } M \text{ is power of } 2, \ \log_2 M \text{ is an integer.} \quad (2.4.2)\ [10]$$

In Phase Shift Keying (PSK), the representation of constellation points can be articulated as:

$$P_m = Ae^{\frac{j\pi(2m-1)}{M}} \quad (2.4.3)\ [10]$$

Usually, for Phase Shift Keying (PSK), the value of M can be 2, denoting Binary PSK or BPSK; 4, representing Quadrature PSK or QPSK; 8, indicative of 8-PSK, and it continues in similar progression [10].

2.4.2. Pulse Shaping

Pulse shaping in data transmission systems hinges on three critical requirements. Firstly, to minimize inter-symbol interference, the chosen pulse shape should ensure zero interference during pulse sampling times. While at the receiver end, pulses are typically centred within their allocated intervals for sampling; the ideal shape should maintain a zero value at the heart of all intervals, except its own. The classic rectangular pulse exemplifies this, but alternatives that remain zero at every other interval's centre are also viable. The second requirement revolves around bandwidth limitations. For adherence, the Fourier transform of the pulse shape should not exceed a specific threshold. Lastly, from a pragmatic standpoint, it is essential that the time-domain pulse tails decay swiftly. This rapid decline safeguards against significant inter-symbol interference that might arise due to unavoidable timing jitters in any transmission system. If these pulse tails linger or don't diminish adequately, then even minor timing discrepancies can lead to notable interference during sampling. The raised cosine pulse is satisfied the requirements and Nyquist's first criterion, so two equivalent forms of often appear in the literature [28]:

$$P(\omega) = \begin{cases} \tau, & 0 \le \omega \le \frac{\pi(1-\alpha)}{\tau} \\ \tau \cos^2\left\{\tau\left[\omega - \frac{\pi(1-\alpha)}{\tau}\right]/4\alpha\right\}, & \frac{\pi(1-\alpha)}{\tau} \le \omega \le \frac{\pi(1+\alpha)}{\tau} \\ 0, & \omega > \frac{\pi(1+\alpha)}{\tau} \end{cases} \quad (2.4.4)\ [28]$$

$$P(\omega) = \begin{cases} \tau, & 0 \le \omega \le \frac{\pi(1-\alpha)}{\tau} \\ \frac{\tau[1-\sin\{\tau(\omega-\pi/\tau)/2\alpha\}]}{2}, & \frac{\pi(1-\alpha)}{\tau} \le \omega \le \frac{\pi(1+\alpha)}{\tau} \\ 0, & \omega > \frac{\pi(1+\alpha)}{\tau}. \end{cases} \quad (2.4.5)\ [28]$$

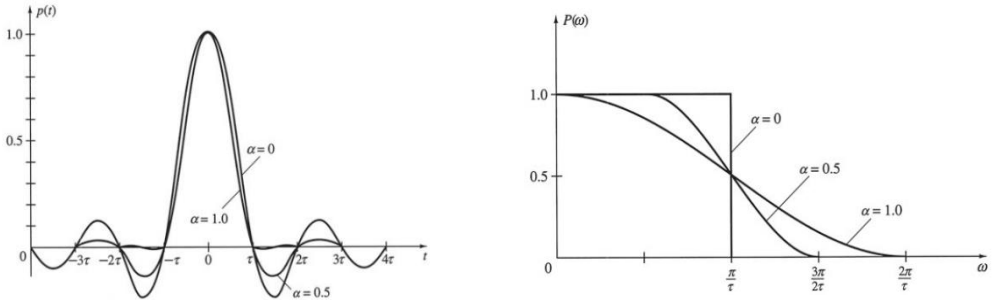

Figure 9 - Raised cosine spectral shaping [28]

From Figure 9, it's evident that the parameter α is crucial. It impacts both the necessary bandwidth and the extent of the tails of p(t), When alpha(α) is set to 1, the tails in p(t) are significantly suppressed, yet the bandwidth maximizes at $\omega_m = (2\pi/\tau)$. Reducing alpha(α) leads to a decline in bandwidth while making the tails of p(t) more noticeable. Typically, alpha's value for data communication is between 0.3 and 1.0, but in advanced systems, it can even be as low as 0.1.

2.4.3. Channel Characteristics

2.4.3.1. AWGN Channel Model

The wireless channel is subject to the noise, frequency and phase offset as described in previous sections. The additive white Gaussian noise (AWGN) can be used to model noise in the wireless channel. The AWGN channel model has three characteristics: additive, white, and Gaussian [10]. The white noise is going to be explained as it is used in the project.

$$c_n(\tau) \stackrel{\text{def}}{=} E(n(t+\tau)n(t)) = \frac{N_0}{2}\delta(\tau) \quad = \quad P_{Wnp}(f) = \frac{N_0}{2} \qquad (2.4.6)\ [10]$$

Consequently, the double-sided Power Spectral Density (PSD) of a white noise as described by above left-hand side equation stands at $N_0/2$, and this remains constant across frequencies (which underscores its "whiteness").

For the same noise, its single-sided PSD is N_0 [10].

Chapter 3 : Methodology

3.1. Introduction

In this section of the report, the work undertaken to achieve the project goals, that is defined in section 1.2 is detailed. First, the appropriate Software-Defined Radio (SDR) devices were selected. Next, these SDR devices were integrated with MATLAB/Simulink for testing and analysis. Simulations were then set up to establish a communication link, essentially creating a downlink end-to-end communication. Lastly, considerations for the proper placement and setup of antennas were addressed. Each of these steps was crucial in progressing towards the main objectives of the project.

3.2. Software-Defined Radio device selection

There several Software-Defined Radio (SDR) devices were widely recognized for their adaptability and performance, making them suitable for applications like beamforming and learning about SDR. Some of them are listed and compared below table.

	HackRF One	**RTL-SDR**	**USRP N210**	**BladeRF xA4**	**PlutoSDR**
Max Frequency	6 GHz	1.7 GHz	6 GHz	6 GHz	3.8 GHz
Bandwidth	20 MHz	2.4 MHz	61.44 MHz	61.44 MHz	20 MHz
Sample Depth	8-bit	8-bit	12-bit	12-bit	12-bit
Duplex	Half	NA	Full	Full	Full
Number of Antennas	1x1	0x1	2x2	2x2	1x1
Price	268 £	40 £	2859 £	425.17 £	232 £
Beamforming Capability	No	No	Yes	Yes	No

Table 1 - SDR Comparison table [29] [30] [31] [32]

The bladeRF xA4 is a robust and advanced SDR platform that's well-suited for beamforming applications. Its capabilities stem from its wide bandwidth, high sample rate, and most notably, its support for MIMO (Multiple-Input Multiple-Output) configurations, which are fundamental for beamforming operations. Having this SDR available in the university setting provides students and researchers an invaluable tool for hands-on exploration and experimentation in beamforming techniques, ensuring that they are working with industry-standard

equipment. On the other hand, for those just beginning their journey in the realm of SDR, the PlutoSDR is an excellent starting point. Notably, it boasts robust support for MATLAB Simulink, a leading environment for simulation and algorithm development. This integration streamlines the process of designing, testing, and implementing SDR-based algorithms. Therefore, the PlutoSDR and BladeRF xA4 is selected because of their suitability and affordable price for this project.

3.3. Integrating the hardware with MATLAB/Simulink

The MATLAB/Simulink platform is selected to create end-to-end communication in this project because MATLAB/Simulink stands as a premier platform for SDR-based end-to-end communication system development, largely due to its comprehensive toolboxes and seamless integration capabilities. Simulink's graphical environment allows users to visualize, design, and simulate entire communication systems, from the baseband algorithms to the RF interface, all within a singular cohesive framework. This holistic approach significantly streamlines the design-to-deployment pipeline. Moreover, MATLAB's extensive built-in libraries and functions facilitate rapid prototyping, enabling users to readily test new concepts or algorithms. When paired with selected SDR devices, MATLAB/Simulink can directly interface with the hardware, allowing real-time signal transmission and reception. This tight integration means that users can swiftly transition from a simulated environment to real-world testing scenarios. Consequently, MATLAB/Simulink offers a unified platform where theory meets practice, making it an optimal choice for developing sophisticated SDR-based communication systems.

3.3.1. Developing MIMO Block for MATLAB/Simulink

The BladeRF platform offers support for MATLAB and Simulink through its binding with the libbladeRF library. LibbladeRF is a C/C++ library designed to provide a direct interface with the bladeRF hardware. However, there is only SISO Simulink block for bladeRF provided by officially. That means bladeRF SDR block in the Simulink does not support 2x2 MIMO communication. In order to overcome this, the steps of BladeRF MIMO block developed for Simulink device will be explained in this section. Development process is done by editing given SISO Simulink files.

3.3.1.1. Understanding of given MATLAB System Object

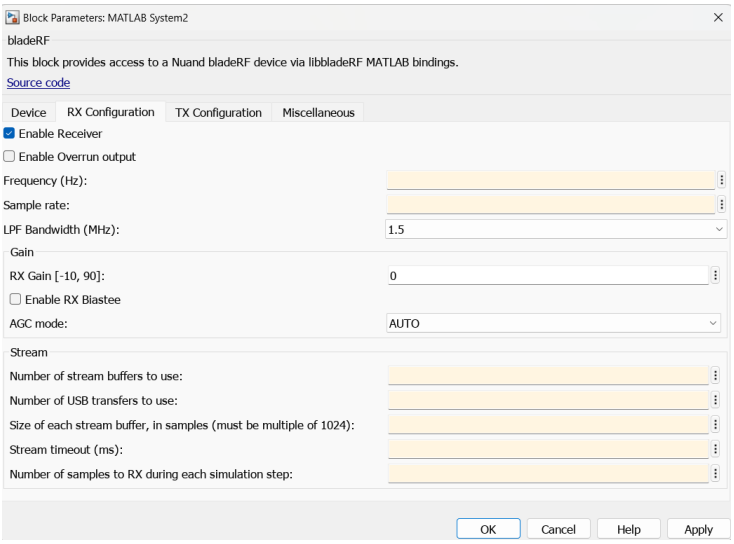

Figure 10 - Simulink user interface

Figure 10 shows the user interface for SISO BladeRF block. The interface enables the user to enter the Rx and Tx parameters such as centre frequency, sample rate and Rx/Tx Gain. After collecting the parameters from the user. The SISO Block call necessary function to initiate hardware for communication when the simulation is started.

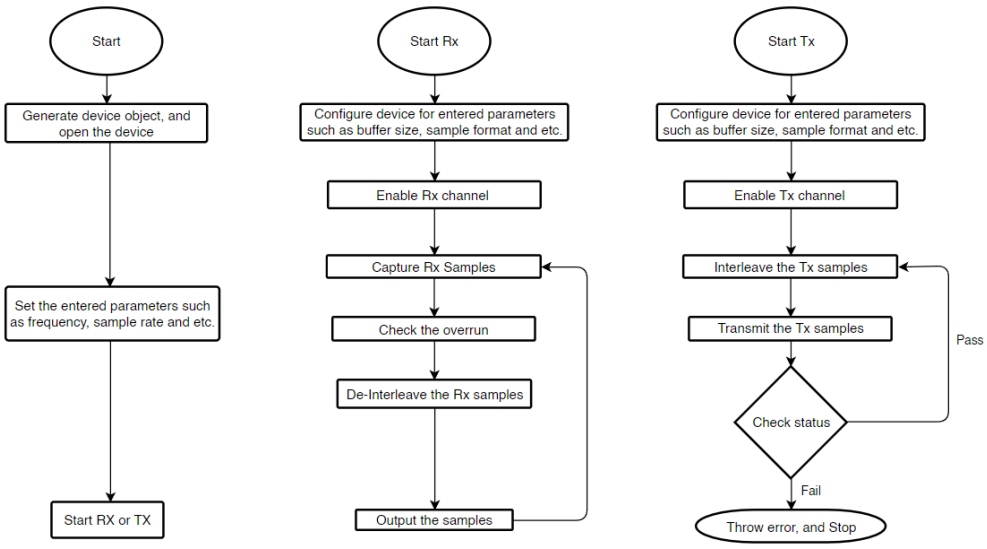

Figure 11 - Flow diagram of the block

Figure 11 illustrate the flowchart of the operations are done in the SISO Simulink block for BladeRF SDR device when the simulation is started. The block calls the functions from official libbladeRF library when it interacts with the SDR device. The given SISO block is associated with several files which is installed by

bladeRF software installer. The installer document is provided in references [33]. The main operations shown in Figure 11 are done by following files: bladeRF.m, bladeRF_simulink.m, bladeRF_XCVR.m and bladeRF_IQCorr.m.

To explain the operations in more detail, for instance, the device is opened by calling “bladerf_open” function in libbladeRF library. Then, the first channel is activated by giving the channel number to the “bladerf_enable_module” function. The whole process will not be described, as one of the main purposes of the report was not to explain these operations.

3.3.1.2. Editing and Developing MATLAB System Object for MIMO Block

To adapt the bladeRF device for MIMO operations, a detailed investigation was undertaken into the provided SISO block files alongside the libbladeRF library and its associated documentation. The in-depth analysis of these resources aimed to uncover the foundational mechanisms and configurations of the SISO settings, offering insights into potential modifications and extensions required to facilitate MIMO configurations. By comprehending the interactions and dependencies between the block files and the libbladeRF library, it became possible to chart a clear developmental pathway towards the creation and implementation of MIMO settings tailored specifically for the bladeRF device.

Figure 12 - User interface and block symbol for MIMO block

Figure 12 shows the developed block and user interface that covers two additional tabs which are Rx2 and Tx2 where user can enter the parameters for second Tx/Rx channel. The user can enable second Rx and Tx channels with or without first Rx and Tx channels, and if both Rx/Tx channels are activated, MIMO settings will be enabled. To enable to MIMO feature, the following files are edited and developed: bladeRF.m, bladeRF_simulink.m, bladeRF_XCVR.m and bladeRF_IQCorr.m. These developed files are provided in appendix A.

3.4. Simulations

In this section of the report, the intricacies of simulations developed in Simulink are elucidated. Initially, the focus is on establishing end-to-end digital communication through the detailing of the QPSK transmitter and receiver structures. This transceiver architecture not only lays out the fundamental communication mechanics but also provides solutions to real-world issues that might be encountered. Following that, the integration of the beamforming technique within wireless communication is explored, shedding light on its implementation and benefits.

3.4.1. QPSK Transmitter and Receiver

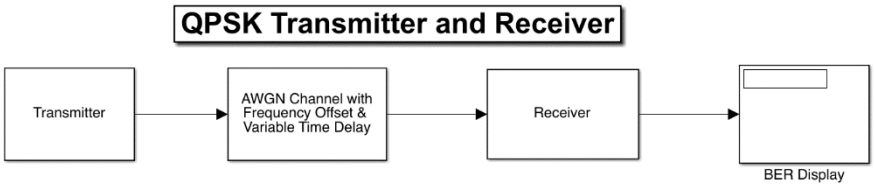

Figure 13 – The overview of QPSK Transceiver structure in Simulink

Figure 13 shows the overview structure of QPSK transmitter and receiver in Simulink. This Simulink model is mainly based on example provided by MATLAB/Simulink in [34]. Each of the element in the communication model is going to be discussed in this section. The shown wireless communication system can be said it is the downlink end-to-end communication.

3.4.1.1. Transmitter side

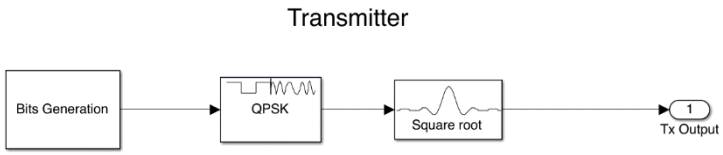

Figure 14 - Transmitter architecture

The background information and their aim of QPSK and Square root (Raised Cosine Filter) blocks in Figure 14 are discussed in section 2.1.3. Bits generation block and whole transmitter chain is going to explained in this part.

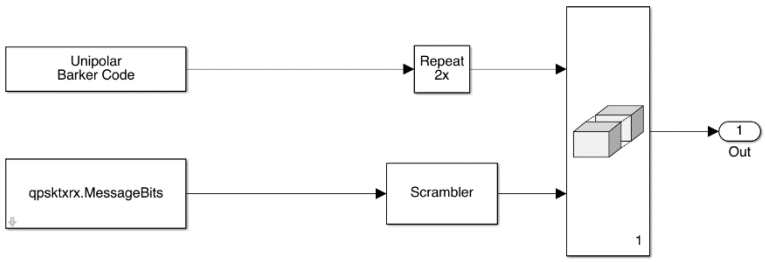

Figure 15 - Inside of Bits Generation block

qpsktxrx.MessageBits block is responsible for the generating bits of the information. A MATLAB Script is created to input each the block's parameters in the simulation, so the script generates the message to be transmitted. In this case, "Hello World" message is generated, and its ASCII codes are converted into bits in the script, then qpsktxrx.MessageBits block samples it with sample time (T_{SM}). After that, Scrambler block is used to ensures that the transmitted data appears random and uncorrelated, which helps to mitigate the effects of interference and improve the overall reliability of the communication system [35]. In addition, the scrambled data is combined with 13-bit Barker code oversampled by two because Barker code is commonly used for frame synchronization in digital communication, and it is a sort of binary pseudo-random code [36].

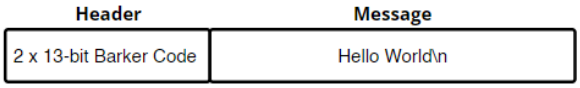

Figure 16 - Frame structure

Figure 16 shows the frame structure used in system. 26-bit Barker Code and 84-bit long "Hello World\n" which contains 12 characters. Hence, the frame size is $26 + 84 = 110\ bit$.

3.4.1.2. Channel Modelling

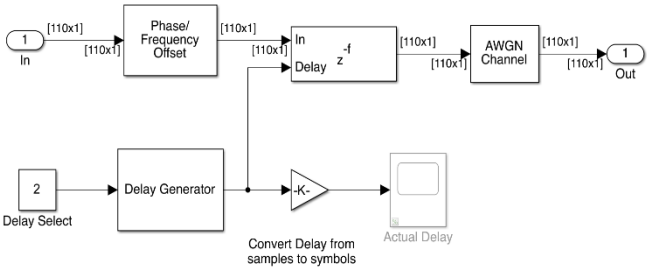

Figure 17 - AWGN Channel with frequency offset and variable time delay

Figure 17 shows the channel model structure. The example offers to the designer to modify the frequency shift value and time delay created to simulate channel impairment in order to see the effect on the receiver side after symbol synchronizer and carrier synchronizer.

3.4.1.3. Receiver side

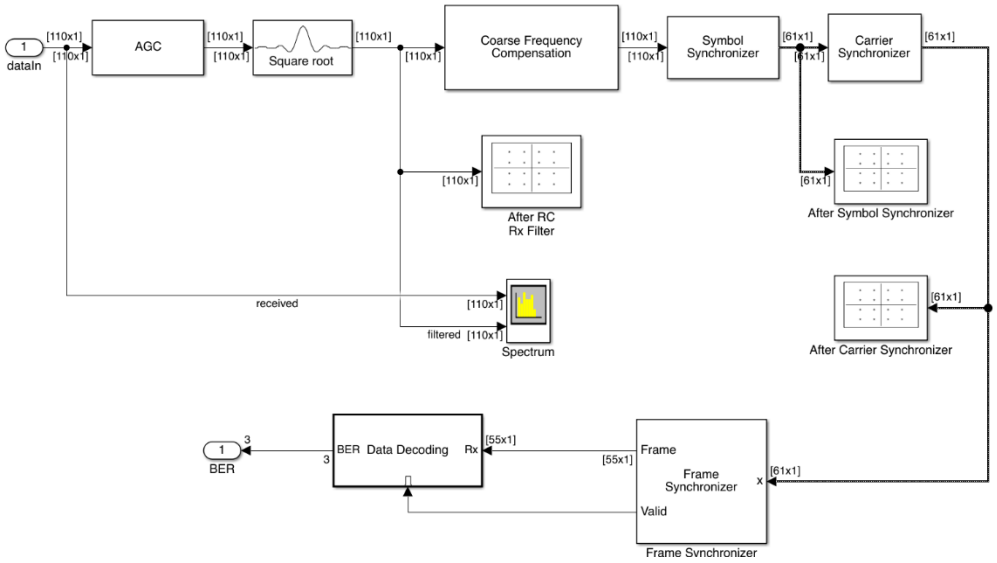

Figure 18 - Receiver architecture

Figure 18 represents the blocks used in receiver side to decode received message successfully. The technical background and aim of the blocks are discussed in the section 2.1.3. **The Coarse Frequency Compensation** part helps fix the input signal using a basic guess of the frequency error. It guesses the error by averaging numbers from the Coarse Frequency Compensator block. The Phase/Frequency Offset block then makes the needed changes. Even after this fix, there's often a small remaining error that can cause a slow rotation of the constellation. The Carrier Synchronizer block helps correct this small leftover error [34]. **The Symbol Synchronizer block** handles timing recovery by using a PLL to fix timing mistakes in the received signal. This block guesses the timing mistake with the help of the Gardner algorithm, which works the same way regardless of its position relative to frequency offset fixes [34]. **The Carrier Synchronizer block** handles the detailed frequency adjustments. It uses a phase-locked loop (PLL) to follow and correct small remaining frequency and phase mistakes in the input. This PLL uses a Direct Digital Synthesizer (DDS) to make the correction needed to balance out these small mistakes. The correction amount from the DDS is based on adding up the error amounts given by a Loop Filter [34]. The MATLAB System block handles frame synchronization using a **Frame Synchronizer** System object™. This block looks for a known frame header (a QPSK version of the

Barker code) in the received QPSK symbols to figure out where the frame header is. With this location info, it properly lines up the frame edges. It also changes the changing-size output from the Symbol Synchronizer block into a set size, which is needed for the next steps. The block's second output tells if the first output is a correct frame with the right header, and if yes, it lets the Data Decoding part work [34].

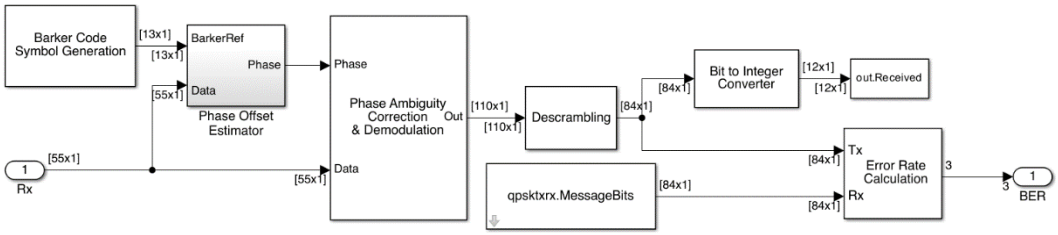

Figure 19 - Inside of Data Decoding block

The Data Decoding system, when activated, handles clarifying phase uncertainty, demodulation, and decoding text messages. The Carrier Synchronizer block might connect to the unmodified carrier with a phase change of 0, 90, 180, or 270 degrees, leading to uncertainty about the phase. The Phase Offset Estimator system figures out this phase change. The Phase Ambiguity Correction & Demodulation system adjusts the input signal based on the guessed phase change and processes the fixed data. The main data bits are then sorted out and displayed [34].

3.4.1.4. Simulation Results

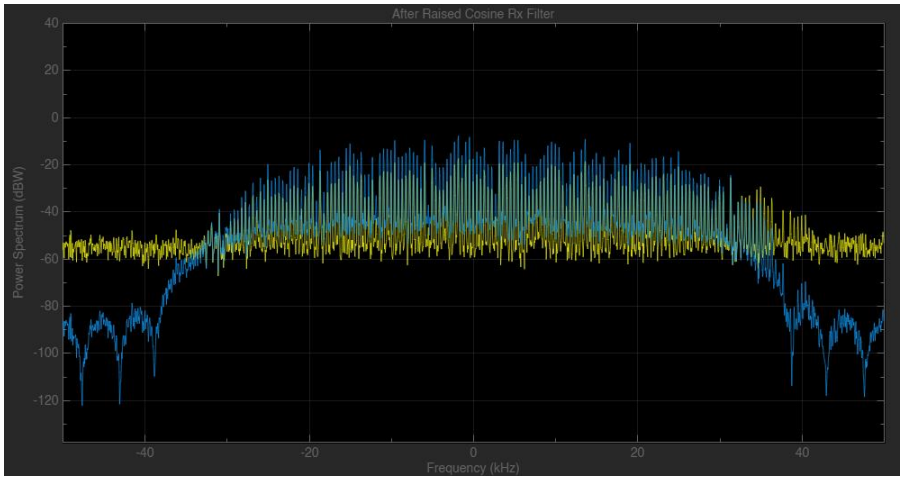

Figure 20 - Spectrum after Raised Cosine Rx Filter

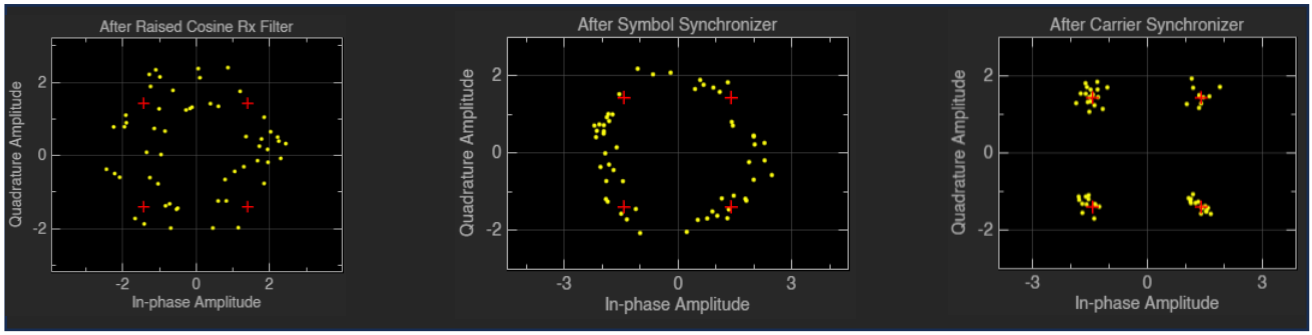

Figure 21 - Effect of Symbol and Carrier Synchronizer on the Constellation Diagram

Figure 21 shows the three different Constellation diagram, response of the received signal, after symbol synchronizer, and after carrier synchronizer are shown respectively. It can be seen that spread out points(symbols) aligned to form a circle after symbol synchronizer, but the points still have rotation due to carrier off-set. Carrier synchronizer eliminates the rotation and aligns the received symbols with expected positions.

3.4.2. Beamforming Integration

The MATLAB/Simulink offers several built-in beamforming algorithms as block such as Frost beamformer, GSC beamformer, LCMV beamformer, MVDR beamformer, and phase shift beamformer. Among the many algorithms, the Frost and Generalized Sidelobe Canceller (GSC) beamformers are adaptive methods, with Frost focusing on least mean squares optimization and GSC separating desired signals from interference for efficient noise cancellation. The Linearly Constrained Minimum Variance (LCMV) and Minimum Variance Distortionless Response (MVDR) beamformers, also adaptive, work by placing nulls in interference directions and ensuring distortionless response in desired directions, respectively. They provide enhanced resolution but can be computationally intensive. On the other hand, the Phase Shift beamformer, a conventional method, applies fixed phase shifts to steer the beam, offering simplicity but less adaptability to interference. While adaptive beamformers excel in complex environments, their computational demands can be a drawback. Conversely, conventional beamformers are efficient but may not handle interference as effectively [37]. In this project, MVDR adaptive beamformer is used at transmitter and receiver side because of its interference cancellation feature and computational efficiency with few numbers of antennas.

3.4.2.1. MVDR Adaptive Beamformer

Beamforming aims to guess a desired signal by mixing data from a group of sensors/antennas. Think of it like trying to get a certain flavour by blending different ingredients together. A set of "weights" is used, similar to the amount of each ingredient, to achieve the desired signal. A particular type of beamformer, called the MVDR, works by reducing noise as much as possible while ensuring the main signal remains strong in a specific direction. The best "weights" for this are found by solving following equation:

$$\min_{\mathbf{w}} \mathbf{w}^H \mathbf{Q} \mathbf{w} \;\; s.t. \;\; \mathbf{w}^H \mathbf{d} = 1, \quad \text{where} \tag{3.4.2 [38]}$$

$$\begin{aligned} \mathbf{N}_c(\omega) &= \mathbf{H}(\omega) S(\omega) + \mathbf{N}(\omega), \\ \mathbf{Q}(\omega) &= E[\mathbf{N}_c(\omega) \mathbf{N}_c^H(\omega)] \end{aligned} \tag{3.4.3 [38]}$$

Nc(ω) represents the total noise, which includes reflected paths and other extra sources. Q(ω) is like a data table that shows how this noise interacts. This table is made based on actual data, so it gives clues about where the interference is coming from and how the sensors impact these sources.

Equation 3.4.2 has also elegant closed-form solution:

$$\mathbf{w} = \frac{\mathbf{Q}^{-1}\mathbf{d}}{\mathbf{d}^H \mathbf{Q}^{-1} \mathbf{d}} \tag{3.4.4 [38]}$$

3.4.2.2. Simulation Diagram of Transmitter side

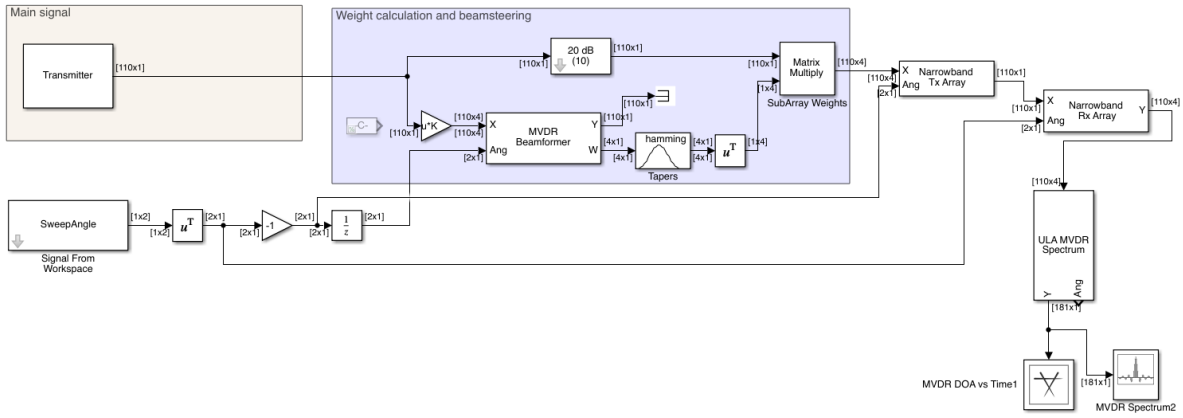

Figure 22 - MVDR Beamformer at transmitter side

Figure 22 shows the created system for MVDR beamforming at the transmitter side. Transmitter side has same structure described in section 3.4.1.

After generating the signal to be transmitted, MVDR block in the purple area calculates the weights to steer main beam towards specified angle. In addition, hamming taper can be used to reduce sidelobes of the beam. The main signal is multiplied by the beamformer weights then transmitted to calculate of its angle of arrival. A scenario was set up in such a way that the angle of the signal to be transmitted changes over time and the angle of arrival was developed to be from 0 degree to 60 degree, and again to the 0 degree.

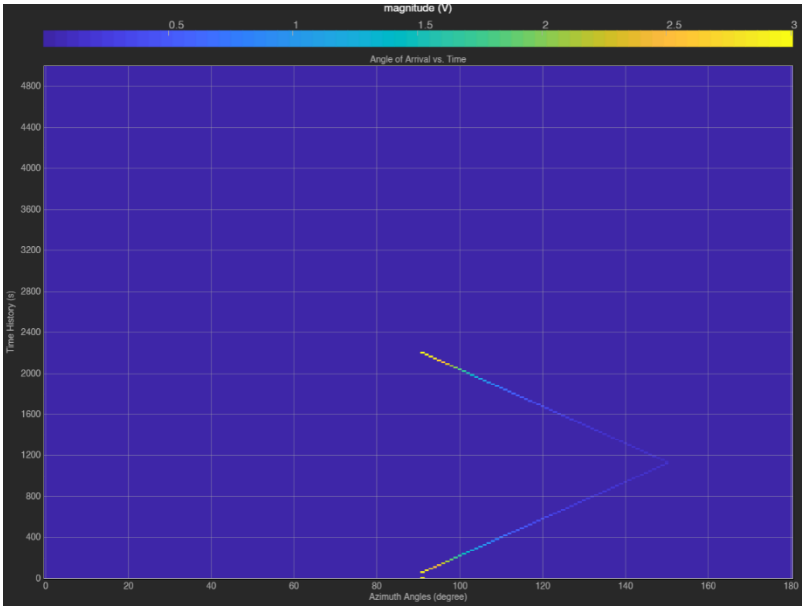

Figure 23 - Angle vs Time Scope

The Angle-Time Intensity tool in Figure 23 shows how the space-based spectrum shifts over time, which indicates the direction from which a signal is coming. When using the MVDR algorithm to estimate this spectrum, it proves that the angle goes from 0 degree to 60 degree and back to 0 degree again.

3.4.2.3. Simulation Diagram of Receiver side

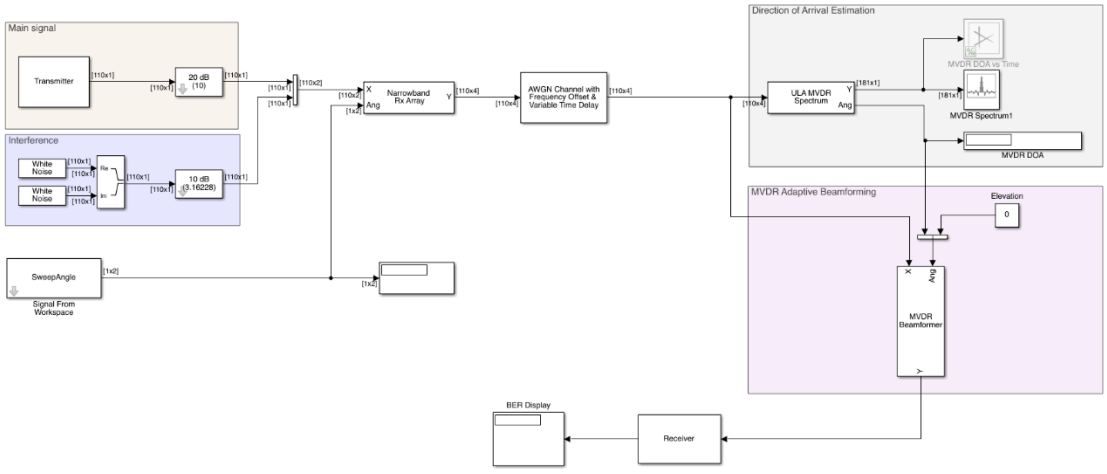

Figure 24 - Direction of Arrival Estimation and MVDR Adaptive Beamforming at Receiver side

Figure 23 represents the MVDR beamforming structure at the receiver side, the simulation has two signals receiving which are desired main signal to be transmitted, and unwanted interference signal consist of noise. The main signal moves from 0-degree azimuth to 45 degrees and back. The interference signal with less power moves opposite direction -45-degree azimuth to 0 and back. After simulating the reception of the signals and adding channel impairments, the ULA MVDR block calculates only azimuth because ULA has symmetry around its central axis, so a DOA method can't distinctively figure out both the horizontal direction (azimuth) and the vertical angle (elevation). After that MVDR beamformer block receives only signal with given angle and transfers it to the receiver which is described in 3.4.1.

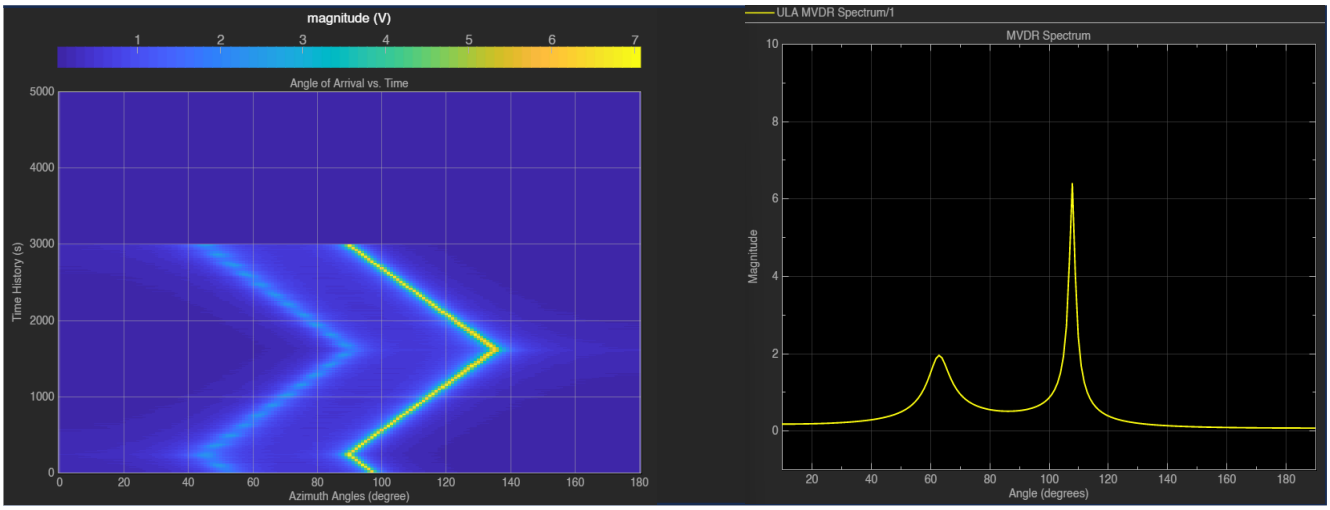

Figure 25 – Angle vs Time Scope and MVDR Spectrum

The Angle-Time Intensity and MVDR Spectrum is shown in Figure 25. The scopes have 90 degrees offset and the range of the scanning range is between -90 to 90 degrees. The Angle-Time Intensity graph shown on the left-hand side proves that the main and noise signals' direction of arrival angles successfully estimated. On the right-hand side MVDR DOA spectrum is shown and main signal is shown with high power and interference signal can be seen with less power.

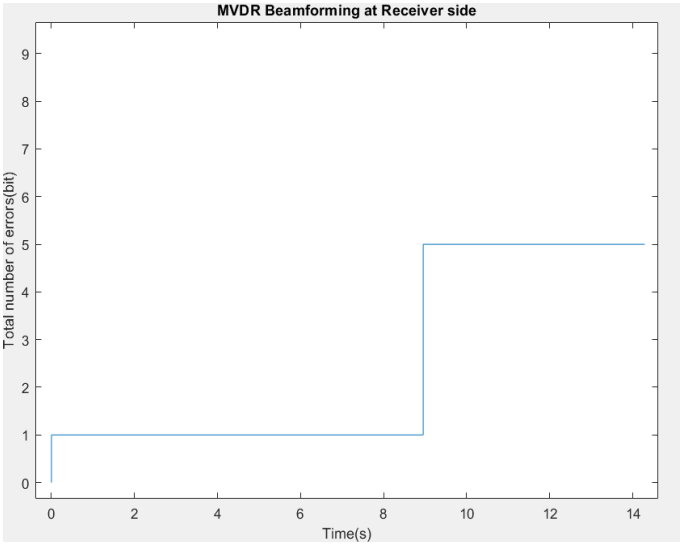

Figure 26 – # of Errors vs Time

Figure 26 on the left-hand side shows the number of errors vs time graph. The simulation was stopped when the total number of bits reached $1e^7$. The graph clearly indicates communication systems successfully has been created with MVDR Beamforming at the receiver side.

3.4.2.4. Downlink end-to-end wireless communication system with MVDR beamforming

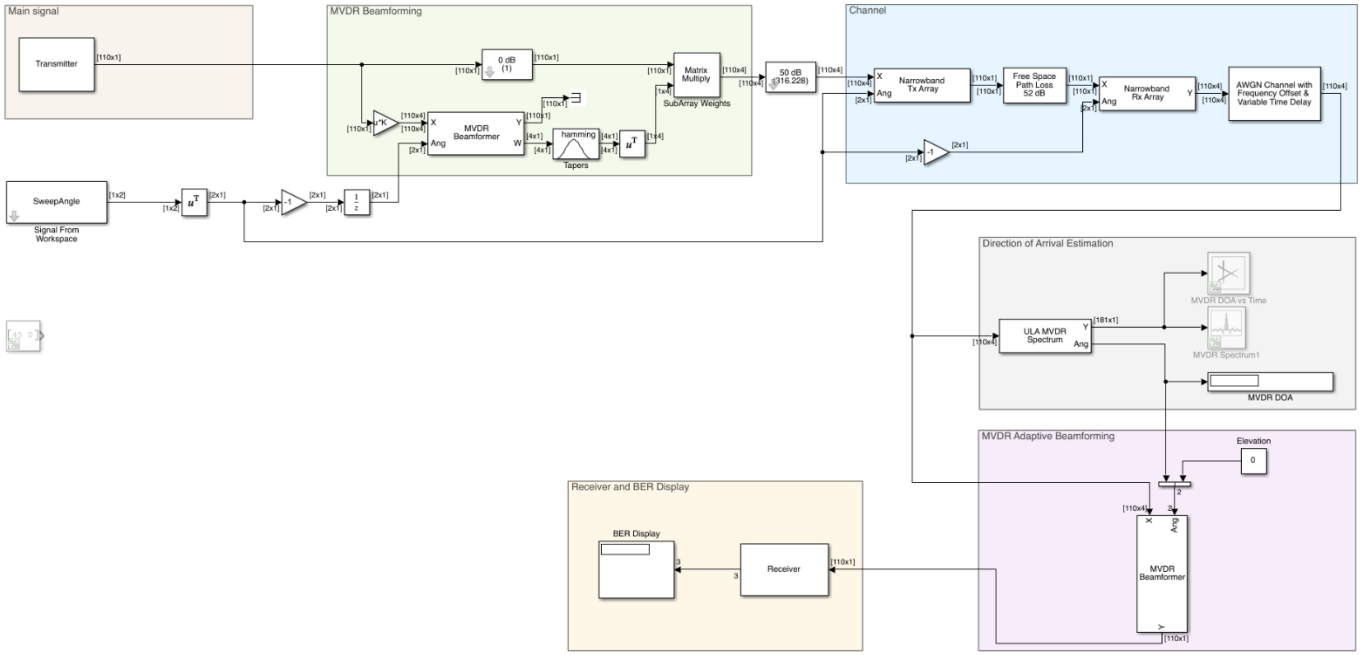

Figure 27 - Wireless communication with MVDR Beamforming at both sides

The transmitter side in section 3.4.2.2 and the receiver side in section 3.4.2.3 is combined to create in order to simulate wireless communication system.

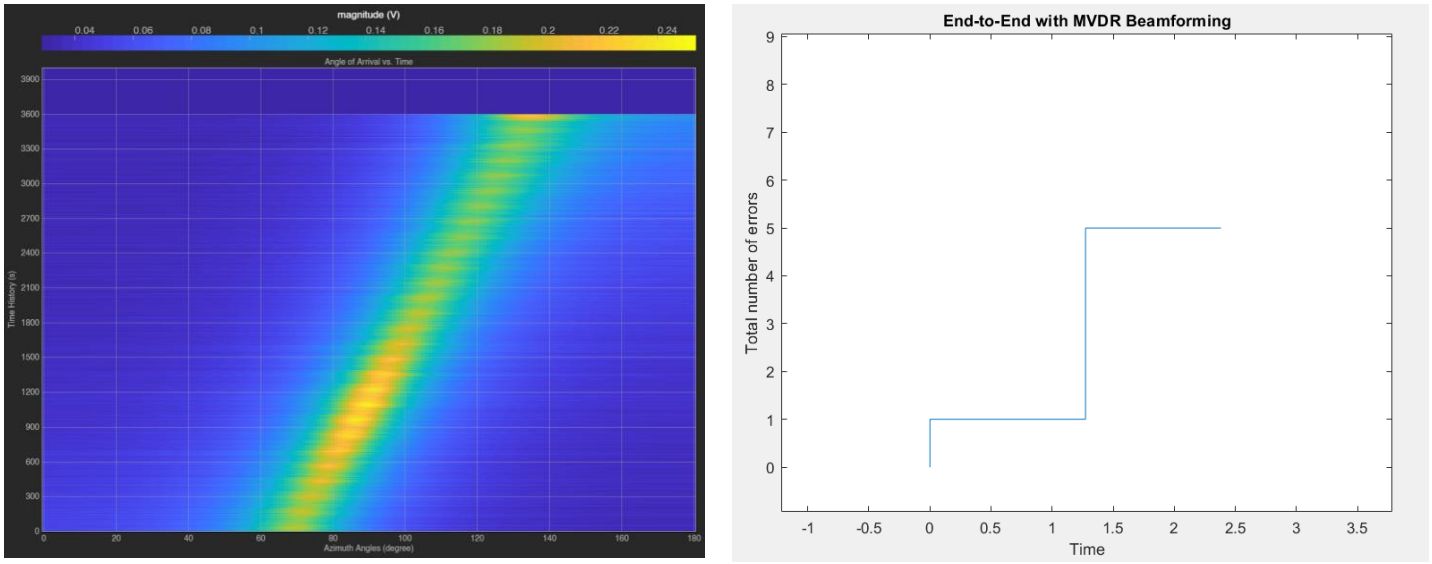

Figure 28 - DoA(azimuth) vs Time and # of errors vs Time graphs

Figure 28 shows the change of direction of arrival azimuth angle over time, and also at the right-hand side the total number of errors(bits) vs Time(s) graph. The sweep angle scenario is that the DOA azimuth moves 45 degrees to -45 degrees and back, so it can be proven on the left-hand side graph. On the other hand, on the right-hand side graph, it can be said that the wireless communication is successfully created because the messages are transmitted successfully. More experiments will be discussed in the discussion part.

3.5. End-to-End communication with beamforming in SDR

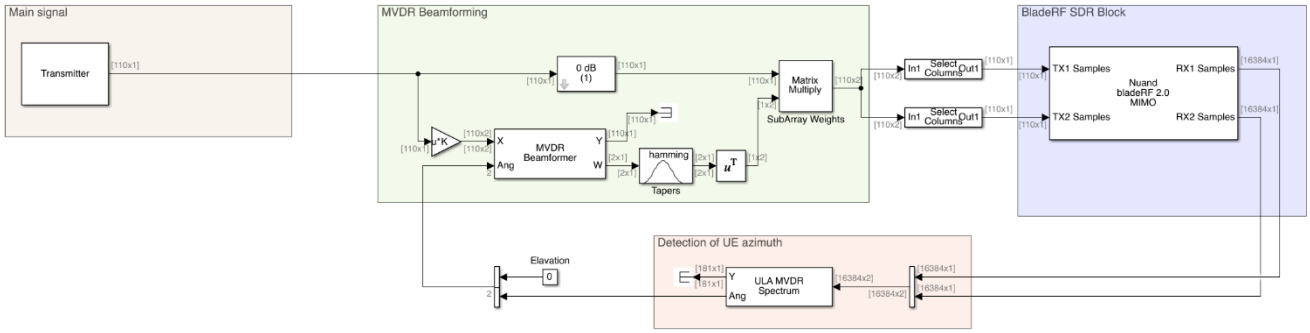

Figure 29 - Transmitter side of practical implementation

Figure 29 illustrates the transmitter architecture of practical implementation of the wireless communication system. Transmitter, MVDR beamformer and DoA estimation parts are described in earlier sections. Detection of UE azimuth part is added to locate receiver side (User Equipment) in order to steer beam towards to the receiver. The assumption of this project is that elevation degree is always zero degree.

In order to use receiver channels in developed bladeRF MIMO block, the FPGA Image version must be v11 or earlier version because Nuand(the manufacturer company) introduces new feature that causes a problem in MIMO communication in the FPGA after version 11 .

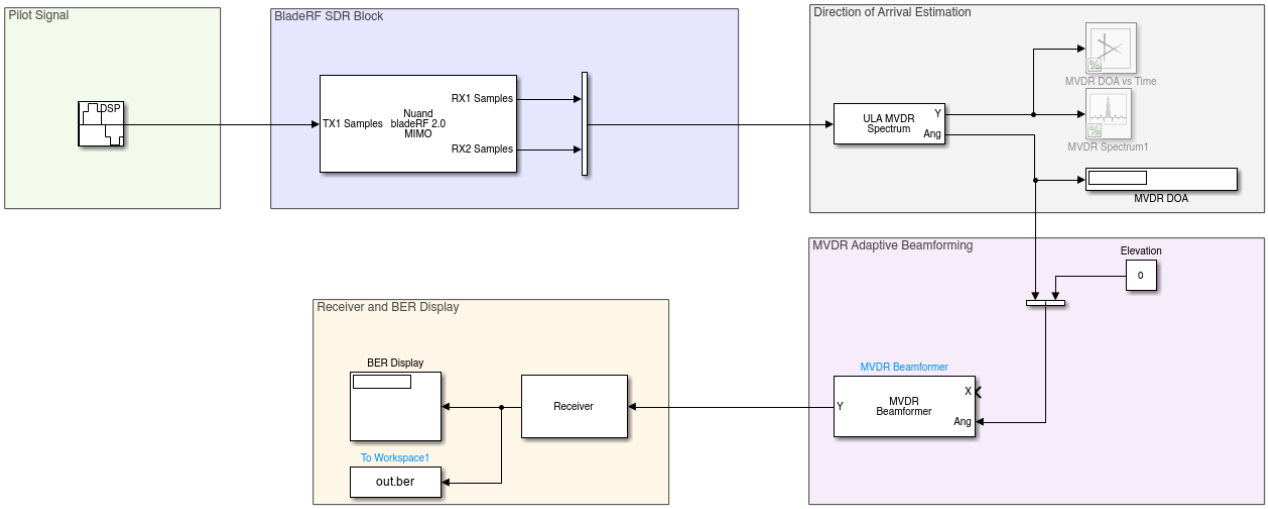

Figure 30 - Receiver side of practical implementation

Figure 30 shows the receiver side of implementation, each block is described in previous sections except pilot signal. The pilot signal is added for the transmitter side to learn the location of the receiver, it does not carry information.

3.6. Antenna Array Design

Beamforming algorithms and DoA estimation requires antenna array design that includes distance between antennas. The spacing between the antennas in a beamforming array affects the beam width and direction of the beams, as well as the potential for grating lobes (unwanted directions where the array produces strong beams). The most common considerations about spacing relate to the half-wavelength rule to avoid the introduction of grating lobes. Some of the important parameters to be considered are listed as follows [39]:

Half-Wavelength Rule: To avoid grating lobes in the visible space, the antenna spacing (d) is often chosen to be less than or equal to half the wavelength:

$$d \leq \frac{\lambda}{2} \quad where,$$

$$\lambda = \frac{c}{f} \qquad c\ is\ the\ speed\ of\ light\ in\ free\ space, approximately\ 3x10^8\ \frac{m}{s}, f\ is\ frequency$$

Grating Lobes: Grating lobes will appear when the spacing exceeds half a wavelength and when the beam is steered. For linear arrays, the condition for the absence of grating lobes when steering the beam to an angle θ is:

$$d \leq \frac{\lambda}{(1 + |\sin(\theta)|)}$$

Array Factor: For linear arrays, the array factor (AF) which determines the beam pattern is given by:

$$AF(\theta) = \sum_{n=0}^{N-1} I_n e^{j\left(2\pi\frac{d}{\lambda} n \sin(\theta) + \phi_n\right)}$$

N is the number of antennas in the array.

I_n is the current amplitude of the nth antenna.

ϕ_n is the phase shift introduced to the nth antenna.

θ is the angle off from broadside (0°).

Beam Steering: To steer the main beam to a desired angle θ, a phase shift is applied across the antennas:

$\Delta\phi = -2\pi\frac{d}{\lambda}\sin(\theta)$ Where $\Delta\phi$ is the phase difference between adjacent antennas.

Beamwidth: The main lobe beamwidth is inversely proportional to the total length of the array. The approximate beamwidth (in degrees) for a uniformly excited linear array is given by:

$BW \approx \frac{2\lambda}{dN}$, where N is the number of antenna elements.

According to given information, an antenna holder platform is designed. Antenna array spacing is designed as 5 cm, so $f_{max} = \frac{3*10^8}{2*(0.05)} = 3\ GHz$. The reason to select 5 cm distancing between antenna because the physical used antennas support 700 MHz to 2600 MHz frequency range. Therefore, the frequency range can be freely used without grating lobes [40].

Figure 31 - 3D view of antenna holder and real antenna mounting

Figure 31 shows the real-world of designed antenna holder with antennas. Two receiver and two transmitter antennas are mounted to each antenna holder and each antenna is connected to the SDR device with Female SMA to Male SMA Coaxial Cable (300mm).

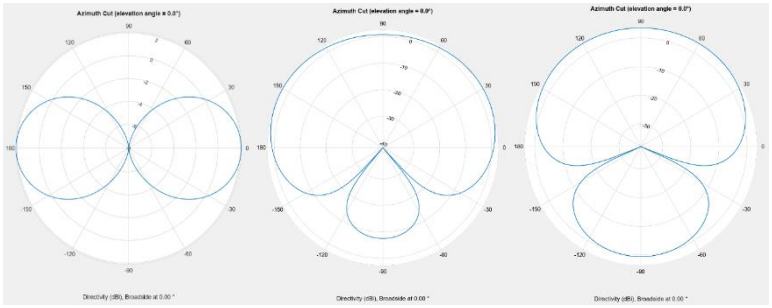

Figure 32 - 2D Azimuth pattern with 2.4 GHz frequency

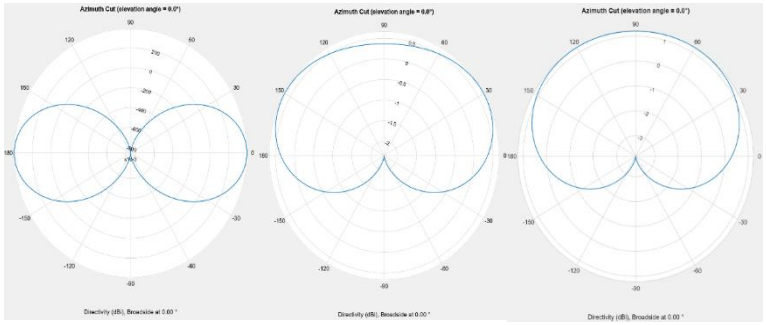

Figure 33 - 2D Azimuth pattern with 1 GHz frequency

Figure 32 and 33 shows the 2D Azimuth patterns with steering angle of 0,30, and 60 degrees. In Figure 32, it can be seen that 2.4GHz frequency cause side lobes when the steering is applied. On the other hand, In Figure 33, 1GHz frequency show better azimuth pattern because it does not create side lobes.

Chapter 4 : Results and Discussion

4.1. Introduction

In this section, the testing and verification is going to be conducted to assess the communication systems highlighted in chapter 3. Every component of the system will be examined to ensure its functionality and performance successful. In other words, the described systems in chapter 3, will be carried out in real world by using BladeRF xA4 SDR devices.

Firstly, the simulation of the QPSK transmitter and receiver in section 3.4.1 will be subjected to practical testing, utilizing a real channel in the practical environment. Subsequently, the constellation diagrams, spectrum, and BER will be analysed and discussed. Secondly, the developed MIMO Simulink block for BladeRF SDR device described in section 3.3.1 will undergo a comprehensive testing phase. This is imperative to validate its functionality and ensure it operates seamlessly. Thirdly, end-to-end QPSK wireless communication with MVDR beamformer is going to be tested practically in different scenarios.

4.2. SISO QPSK Wireless Communication

The described QPSK transmitter and receiver in section 3.4.1 have been split into two as transmitter and receiver. Two MATLAB/Simulink sessions are initialized to ensure real-time process because standard version of MATLAB/Simulink not very well suitable for real-time process. For example, the receiver side can receive data before processing the previous data and it is called “overrun” in this report.

Parameter	Value
Carrier Frequency (f_c)	1 GHz
Number of antennas (N_t , N_r)	1
Sample Rate (f_s)	$R_{sym} * L$ = 600 kHz
Samples per simulation	110
Symbol Rate (R_{sym})	300 kHz
Interpolation factor (L)	2
Decimation factor (M)	1

Table 2 – General Practical Parameters

Above Table 2 shows the general practical parameters. The sample rate was kept as low as possible because the receiver and transmitter were run on the same computer. In this way, the computational load of the programs is reduced and overrun is avoided.

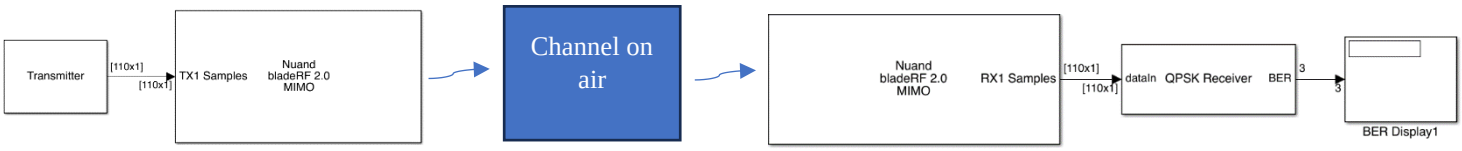

Figure 34 – Illustration of practical QPSK communication with BladeRF SDR devices

Figure 35 represents the QPSK end-to-to wireless communication system, each block was explained in previous sections.

4.2.1. Transmitter Side

The modulator block is simpler in design compared to the receiver block. Thus, its evaluation is primarily based on a constellation diagram, displaying the time and frequecy domain of the generated signals as shown in Figure 35. The parameters of the transmitter are as follows:

Parameter	Value
Raised Cosine: Roll-off	0.5
Raised Cosine: Filter Span	10
Scrambler: Polynomial	$x^4+ x^3+x^2+1$
Scrambler: Initial Condition	0 0 0 0
Bipolar Barker Code	+1 +1 +1 +1 +1 -1 -1 +1 +1 -1 +1 -1 +1

Table 3 - Transmitter side parameters

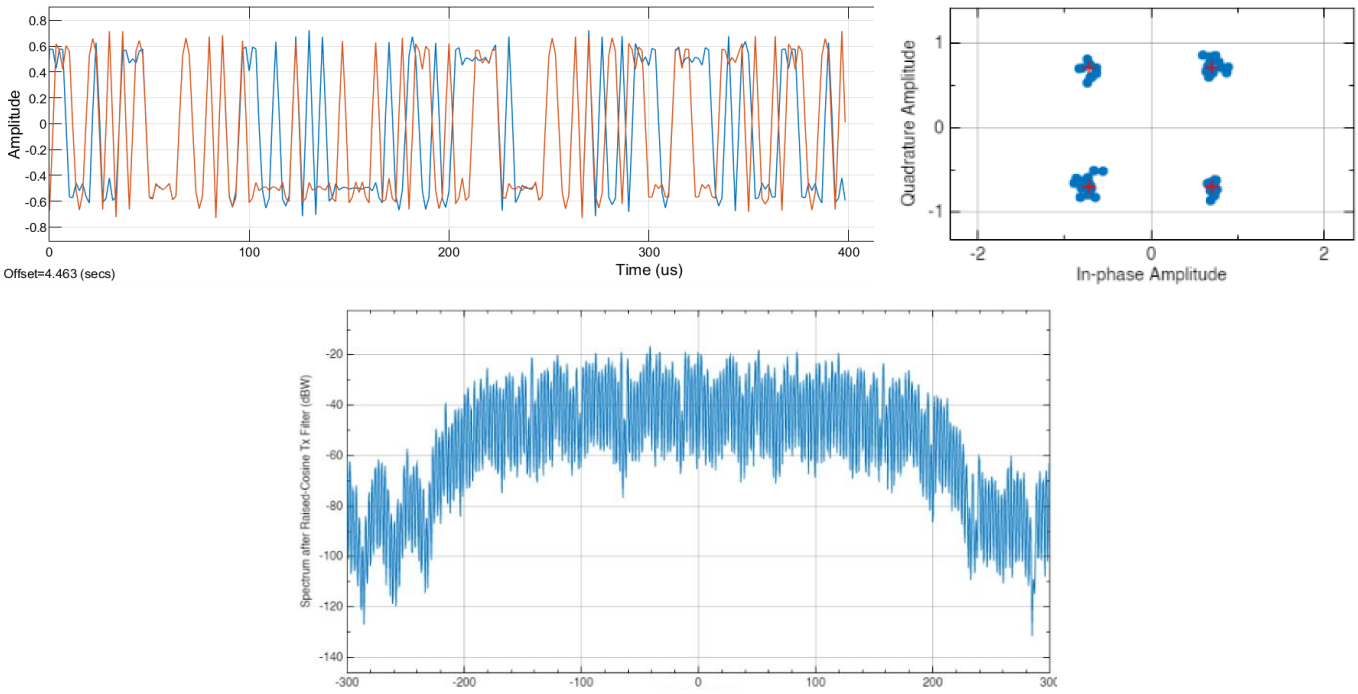

Figure 35 - Time Domain, Frequency Domain, and Constellation diagram of transmitted signal

4.2.2. Receiver Side

In the context of constructing a wireless communication system, Section 2.1.3.3 provides a comprehensive discussion detailing the essential components that should be present on the receiver side. As it is described, the QPSK receiver side especially needs to have matched filter, synchronization (phase and frequency). Therefore, the important parameters are followings:

Parameter	Value
AGC: Time step	0.1
AGC: Desired output power	2
AGC: Averaging length	50
AGC: Maximum power gain	60
Raised Cosine: roll-off	0.3
Raised Cosine: filter span	10
Symbol synchronizer: Samples per symbol	2
Symbol synchronizer: Damping factor	1
Symbol synchronizer: Detector gain	5.4
Symbol synchronizer: Algorithm	Garner (non-data-aided)
Carrier synchronizer: Samples per symbol	2
Carrier synchronizer: Damping factor	1
Frame synchronizer: Detection threshold	0.9

Table 4 - QPSK Receiver side parameters

In the conducted wireless system experiment, both the transmitter and receiver were positioned at a close proximity of approximately 1 meter apart, in an environment characterized by slight scattering. To evaluate the efficacy of the wireless communication in such conditions, constellation diagrams of the received symbols were analysed both pre and post the implementation of carrier and symbol synchronizers. Furthermore, to offer a more comprehensive understanding of the system's performance, a graph illustrating the Bit Error Rate (BER) against time was also provided.

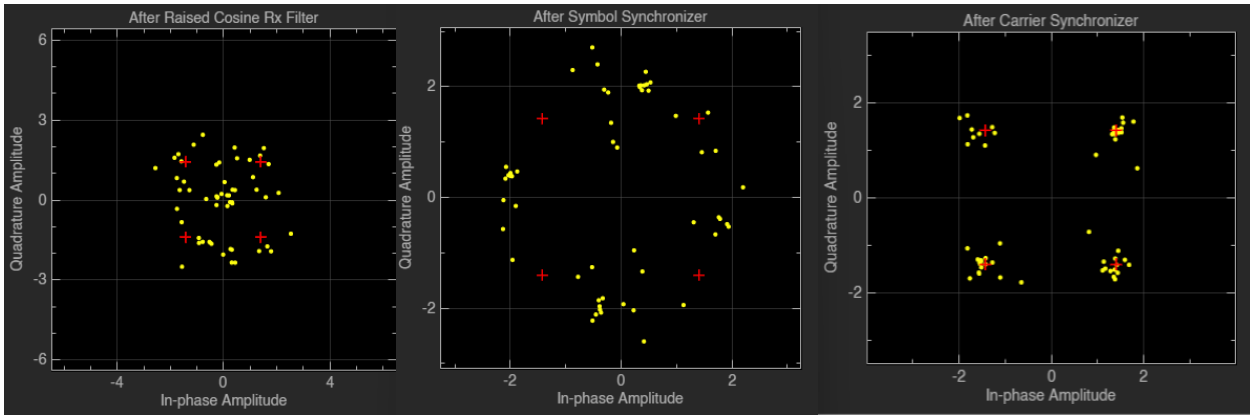

Figure 36 - Constellation diagram of received signal, after symbol synchronizer, and after carrier synchronizer

It can be seen on the left-hand side constellation diagram in Figure 36, the received symbols are hard to distinguish because of the noise, phase offsets, and timing drift. On other words, received symbols are not align with the ideal symbol points. The result of time synchronization can be seen on middle constellation diagram in the figure above. The symbols are now more tightly clustered along the time axis, they are formed as shape of a circle. While the dispersion due to timing errors should be reduced, there might still be a rotation or spreading due to carrier phase and frequency offsets. The carrier synchronizer deals with frequency and phase offsets. Hence, post its application, closely alignment of the symbols to the ideal symbol points in the constellation diagram can be observed on the right-hand side in the figure. Although, most of the symbols are aligned its ideal point, there are some symbols could not be recovered because of non-compensated channel impairments by synchronizers. In addition, as it is mentioned before, unmodulated carriers might be locked on wrong constellation point, but they can be corrected in decoding part where phase ambiguity block is employed.

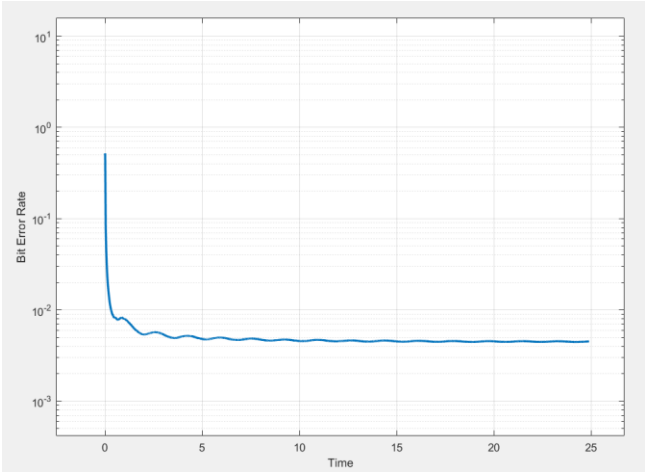


```
□□□ello world
Hello world
Hello world
Hello world
Hem□<Hj□□69
Hello world
Hello world
Hello world
Hello world
Hello world
Hello world
Hello world
Hello world
Hello world
xello world
Hello world
Hello world
Hello world
```

Figure 37 - BER vs Time graph and some decoded messages

4.3. MIMO Block validation

In order to validate the MIMO Simulink block designed for the bladeRF, the identical wireless system as delineated in section 4.2 is utilized for transmitter. However, there is a distinction at the receiver end: the second channel is now activated to facilitate 1x2 communication. At the receiver, both incoming signals are individually processed, undergoing frequency compensation as well as time and frequency synchronization. It's imperative to note that only when both signal frames are confirmed as valid does the system proceed with co-phasing. This co-phasing, along with the subsequent combination of the signals, employs the Equal Gain Combining (EGC) technique. Once harmonized, the received signals are then demodulated to extract the transmitted information.

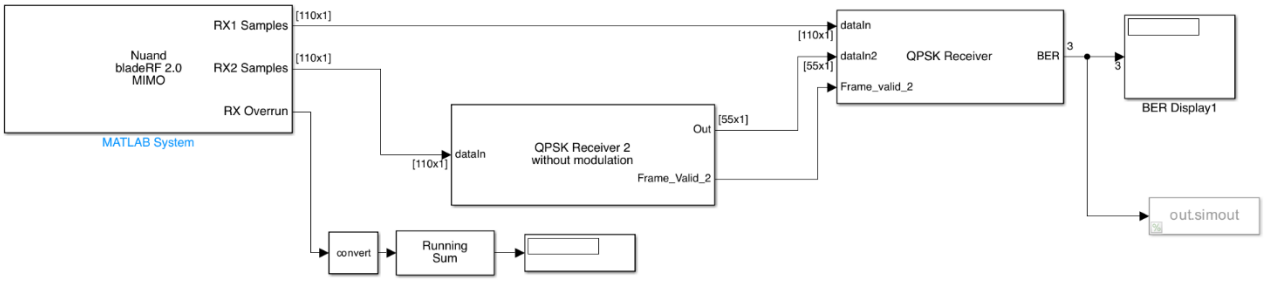

Figure 38 - Receiver side with 2 antennas

The overall receiver architecture is shown in Figure 38, second QPSK receiver is added to correct phase and frequency off-set along with frame synchronization. After synchronization of both branches, they are sent to proceed co-phasing. Figure 39 shows the co-phasing and demodulation of both branches.

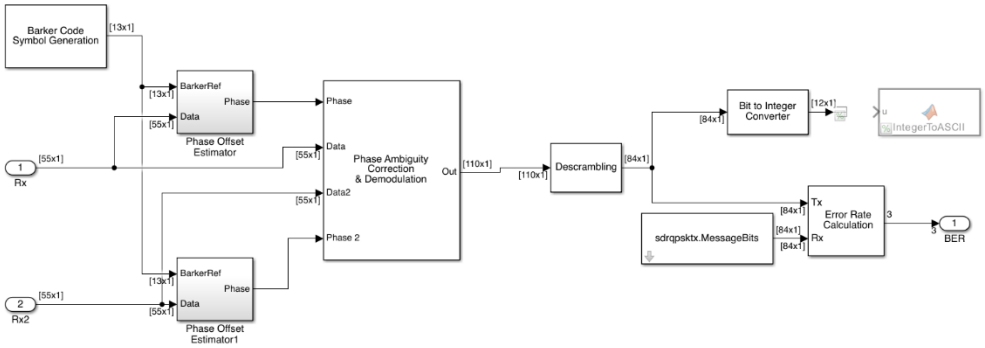

Figure 39 – Phase-offset detection and decoding stage

The co-phasing of the signals is achieved by utilizing the known Barker code embedded in the header of each frame, allowing for precise detection of the phase offset between the two signals. Same reference signal is used to achieve detection of phase-offsets of received two signals. Then, the phase difference between two received

signals are eliminated. After the co-phasing, the signals are summed up to achieve Equal-Gain Combining receiver diversity technique. Finally, combined signal is sent to QPSK demodulation in order to decode received signal.

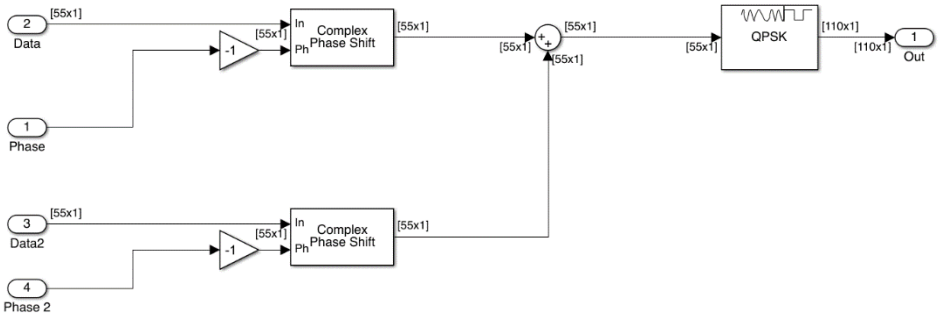

Figure 40 - Co-phasing, EGC and demodulation blocks

To evaluate the impact of the EGC receiver diversity technique, two BER vs. Time graphs were shown below: the first representing a system with EGC utilizing two receiver antennas, and the second depicting a SISO QPSK system without any receive diversity.

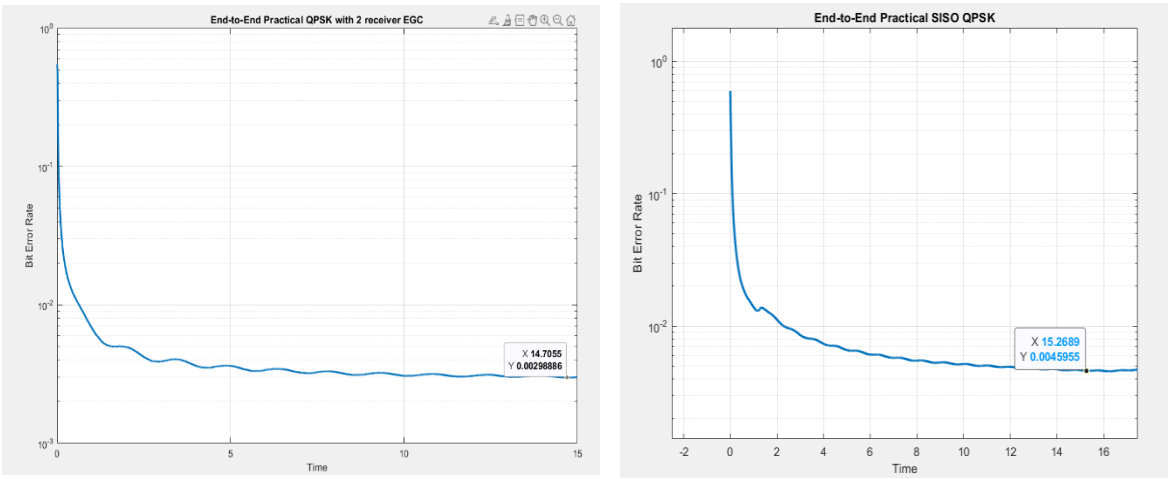

Figure 41 - Comparison of two BER vs Time graph

In Figure 41, two distinct BER vs. Time graphs are presented for scrutiny. On the left-hand side, the graph illustrates the performance of QPSK with the incorporation of two receiver antennas where EGC is actively employed. In contrast, the right-hand side showcases the results for a SISO QPSK system. When examining these graphs under a channel devoid of severe impairments, both seem to exhibit a comparable BER trajectory over time. However, a closer inspection reveals notable differences. The SISO QPSK's BER never descends below the threshold of 0.004, whereas the QPSK system with two receiver antennas and EGC dips beneath a

BER of 0.0029. From this analysis, it can be conclusively stated that the developed MIMO block operates effectively, showcasing its capability to manage multi-channel operations. Furthermore, this comparison validates that the QPSK system, when complemented with two receiver antennas and the EGC technique, outperforms the SISO QPSK in terms of BER.

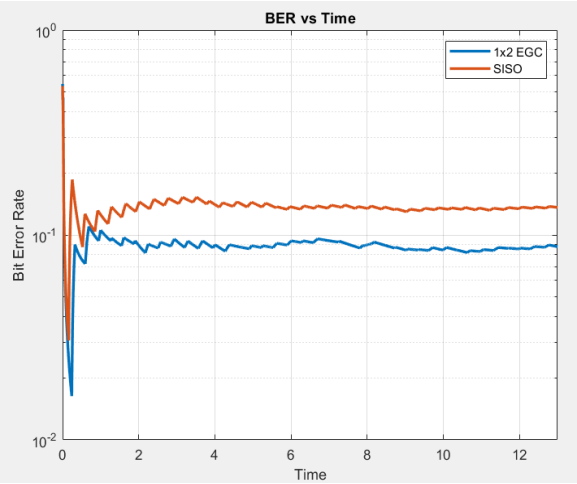

Figure 42 - BER vs Time comparison under Rayleigh flat fading channel

Since the real channel environment cannot be changed, Rayleigh flat fading conditions are applied to the received signals at the receiver side. This way a better comparison can be made on the graph. Figure 42 shows the result of this operation and as expected, the 2-antenna system gives better results. Details and calculations for Rayleigh flat fading are explained in detail in the report of my mobile communication course in Appendix B.

Figure 43 - Real implementation environment

4.4. End-to-End Wireless Communication with Beamforming

Section 3.5 detailed the design of end-to-end wireless communication using MVDR (Minimum Variance Distortionless Response) beamforming, emphasizing real-time computation and minimized latency. Yet, subsequent tests highlighted a significant issue: the execution time on either the receiver or transmitter side exceeded the device's sample rate, leading to overrun or underrun events. As a consequence, the system wasn't equipped to process incoming data rapidly enough, resulting in data loss. The root causes of this latency could be multifaceted. For instance, the BladeRF Simulink block might not have been correctly integrated with the device, or the chosen operating system might not be well-optimized for real-time operations. To solve this problem, some assumptions were made in the system and the algorithms used in the beamforming in section 3.5 were replaced with faster algorithms. Since this is a last-minute problem, I sincerely regret that the report did not focus on the final design.

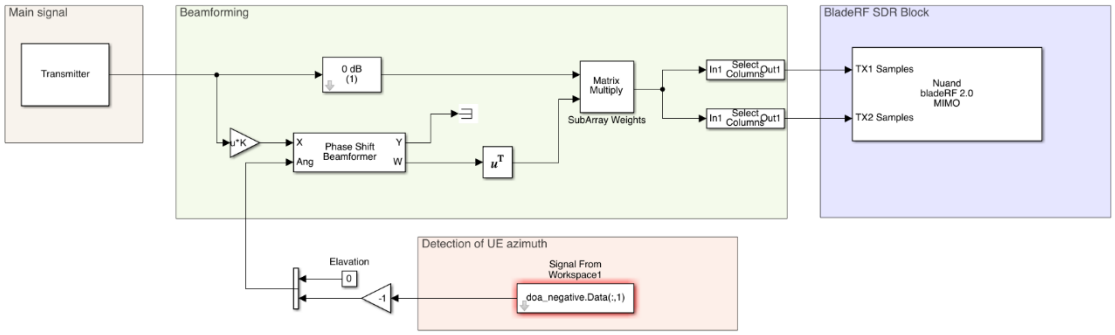

Figure 44 - 2x1 Transmitter Side with Phase Shift Beamformer

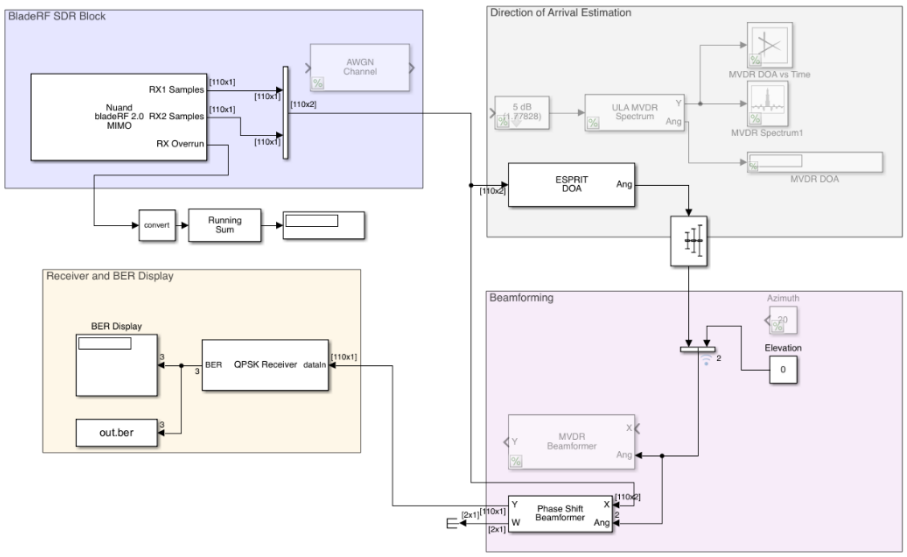

Figure 45 - 1x2 - Receiver Side with Phase Shift Beamformer

Figure 44 shows the 2x1 Transmitter side with Phase Shift beamformer algorithm. The design is almost same in section 3.5 except detection of the receiver azimuth is provided by user. Figure 45 represents the 1x2 receiver with Phase Shift Beamformer where the DOA estimation with ESPRIT algorithm. The design is nearly identical to the design in section 3.5 except that receiver side does not send pilot signal to be detected by transmitter side.

4.4.1. Direction of Arrival Estimation (DOA)

In Figure 45, DoA estimation blocks are shown. The Rx1 and Rx2 samples feds to ESPRIT DoA estimator block and the block produces the estimated DoA angle. However, in practical world with 2 receiver antenna estimation of DoA might be challenging because estimated angle can change rapidly due to channel impairments or higher frequency of carriers. In order to compensate this effect running mean DSP algorithm is used to determine stable and accurate DoA azimuth angle. Figure 46,47 shows the result of DoA estimations, the estimation with running mean block is provides much more stable azimuth angle to the beamformer.

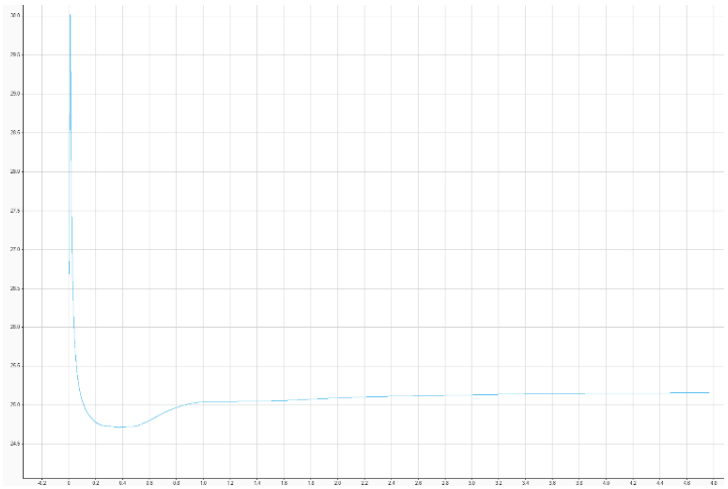

Figure 46 - Azimuth angle vs Time with running mean

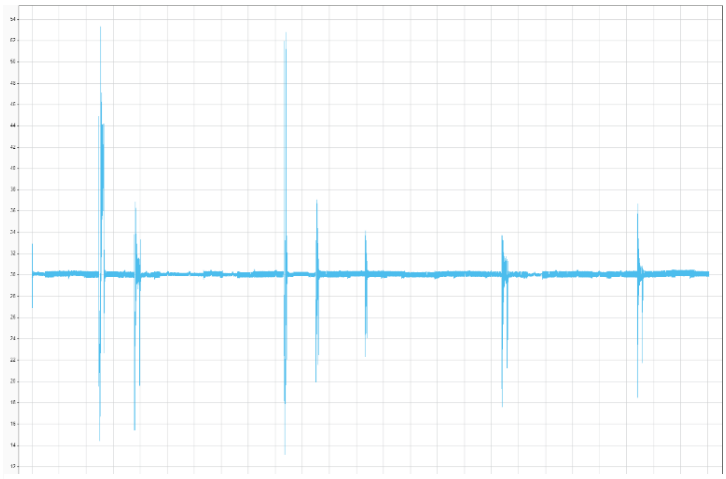

Figure 47 - Azimuth vs Time without running mean

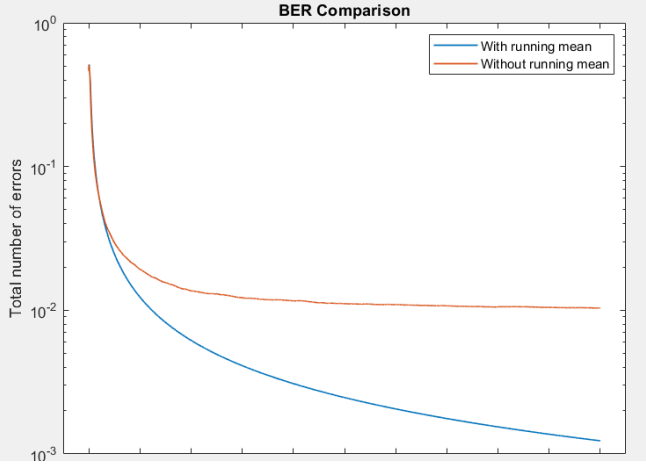

Figure 48 - BER Comparison of two methods

4.4.2. Results with different experiments

In this section, SISO QPSK Transceiver, 1x2 QPSK Receiver diversity with EGC, 1x2 QPSK Beamforming and 2x1 QPSK Beamforming is going to be tested in different scenarios and the results will be discussed. The structure of each wireless system is discussed previous sections, so only the changed parameters are given in this section.

Parameter	**Value**
Center frequency	1.5 GHz
Symbol rate	300 kHz
Tx Gain	50 dB
Rx Gain	40 dB
AGC mode of Rx	Manual
Antenna spacing	10 cm
USB Parameters	***Value***
Number of buffers	32
Number of transfers	16
Buffer size	163840
Timeout	5000 ms

In a controlled experimental setup, three distinct receiver configurations were tested: a Single Input Single Output (SISO) QPSK Receiver, a 1x2 QPSK Receiver utilizing Equal Gain Combining (EGC) for diversity, and a 1x2 QPSK Receiver employing beamforming techniques. These configurations were carefully positioned within the same environment to maintain a consistent relative azimuth angle with respect to each other. To simulate and assess their performance in real-world scenarios, an Additive White Gaussian Noise (AWGN) channel was introduced to each receiver. This allowed for a comprehensive evaluation of the systems under varying signal-to-noise conditions, specifically at 5, 10, and 15 Eb/No levels. This approach provided insights into the resilience and efficiency of each receiver configuration under distinct noise intensities.

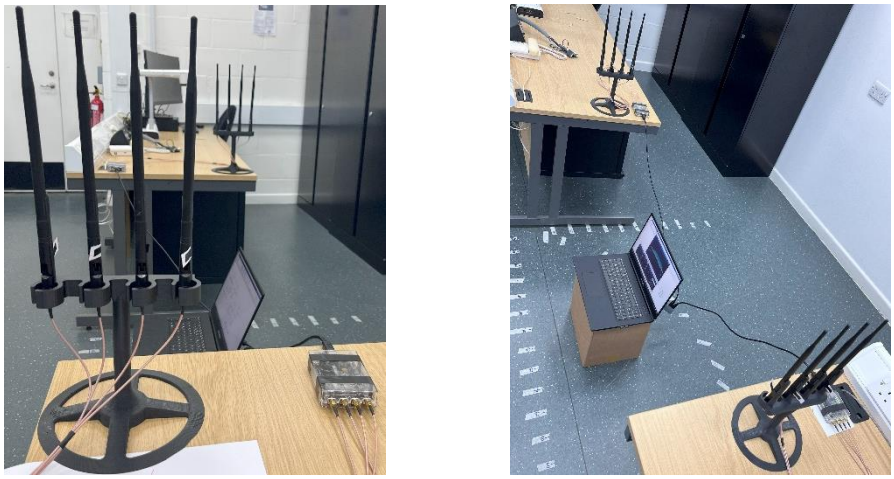

Figure 49 - Real test environment

The transmitter is positioned approximately 40 degrees from the receiver. Figure 50 shows the azimuth vs time graph. This positioning is valid for all tests below.

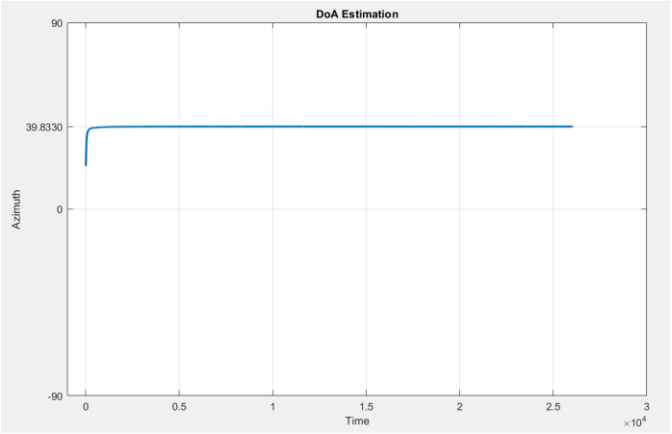

Figure 50 - Azimuth angle of the transmitter relative to receiver

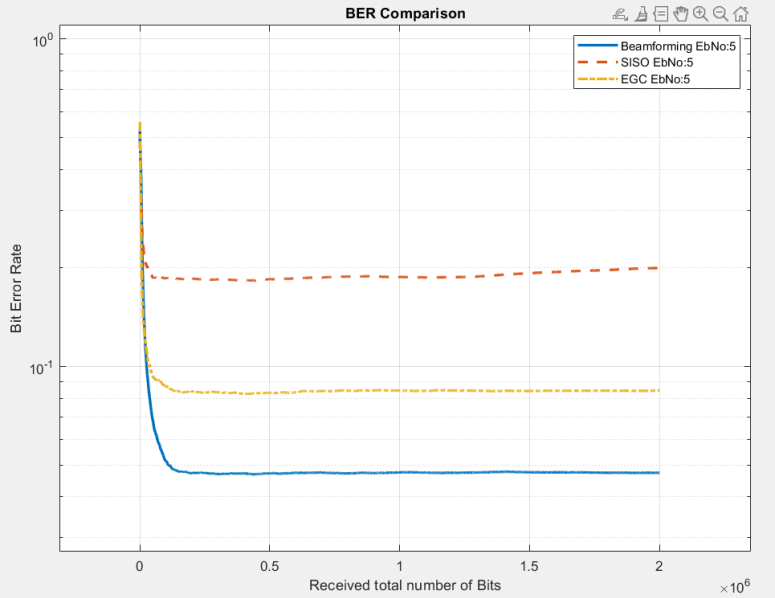

Figure 51 - BER Comparison of three different wireless system with Eb/No: 5 dB

In Figure 51, a clear distinction in performance is evident among the three systems under scrutiny. Specifically, the 1x2 Beamforming system showcases a superior Bit Error Rate (BER) performance when compared to both the 1x2 receive diversity and the SISO system, particularly at an Eb/No value of 5 dB. This comparative advantage underscores the efficacy of the beamforming technique in mitigating the detrimental effects of noise. Therefore, in environments riddled with noise, the beamforming approach demonstrates a pronounced resilience, outperforming both receive diversity and traditional SISO configurations. This superiority suggests that beamforming's spatial selectivity and focused signal reception inherently grant it an edge, especially when operating amidst significant interference or noise.

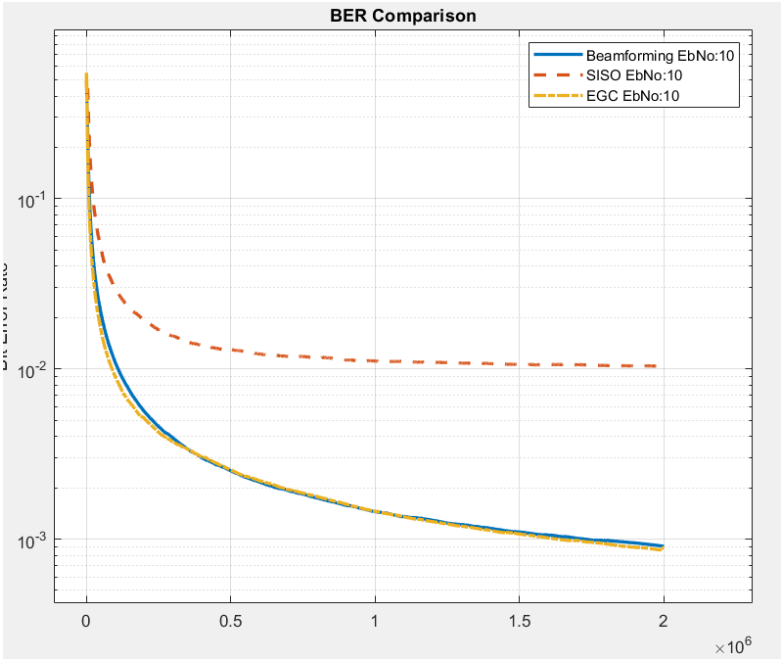

Figure 52 - BER Comparison of three different wireless system with Eb/No: 10 dB

In Figure 52, an interesting pattern emerges in the BER performance among the evaluated systems at an Eb/No of 10 dB. The 1x2 Beamforming system displays a BER curve that aligns closely with that of the 1x2 receive diversity employing EGC, both of which noticeably outpace the performance of the SISO system. This observation underscores the enhanced resilience both beamforming and receive diversity techniques offer in environments with a moderate level of noise. Specifically, while the SISO system struggles to maintain signal integrity amid the noise, both beamforming and 1x2 receive diversity harness their respective strategies — spatial selectivity for beamforming and the collective strength of multiple antennas for receive diversity — to achieve improved noise immunity. Furthermore, in conditions characterized by moderate noise levels, it's evident that beamforming and 1x2 receive diversity might reach a point of performance parity, suggesting that both techniques can be equivalently effective in confronting and mitigating such noise challenges.

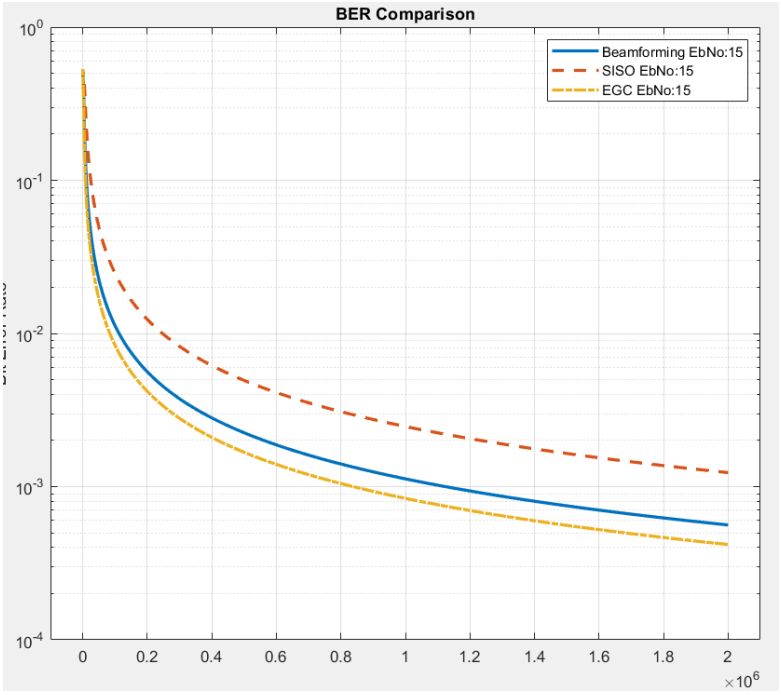

Figure 53 - BER Comparison of three different wireless system with Eb/No: 15 dB

In Figure 53, the BER performance dynamics reveal subtle yet noteworthy distinctions among the three systems at an Eb/No of 15 dB. Notably, the 1x2 Beamforming system, while surpassing the SISO system, lags marginally behind the 1x2 receive diversity utilizing EGC in terms of BER performance. This suggests that in environments with relatively low noise levels, the 1x2 receive diversity employing EGC manages to extract more benefits from its collective antenna system, capitalizing on the combined strength and reduced error probabilities. On the other hand, while the beamforming technique still offers advantages over the traditional SISO configuration, it doesn't quite match the efficacy of the receive diversity in this particular noise scenario. It's plausible that the finer nuances and potential imperfections of the beamforming process become more pronounced in such low-noise conditions. In summary, under the comparatively benign noise challenges presented at an Eb/No of 15 dB, the 1x2 receive diversity with EGC emerges as the more adept strategy, outshining both SISO and beamforming in preserving signal integrity.

4.4.2.1. Integrating interference signal

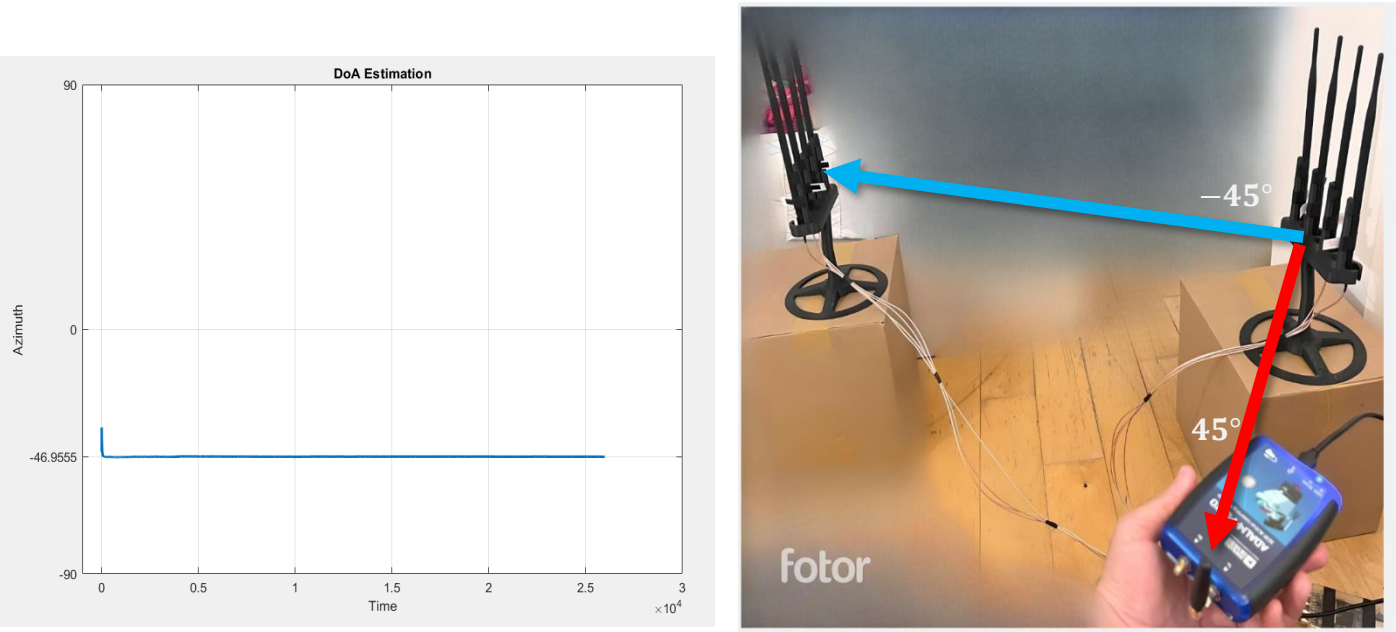

Figure 54 - DoA estimation of the showing practical wireless communication system

In the experimental setup, shown in Figure 55, the receiver is strategically positioned to create specific angular relationships with the transmitting devices. Specifically, it is oriented such that it has a -45-degree angle relative to the bladeRF transmitter device's antennas. This orientation facilitates a particular directional interaction with the bladeRF's emitted signals. In contrast, the receiver is placed at a 45-degree angle to the ADALM-Pluto device's antenna. The ADALM-Pluto device, in this context, is tasked with generating an interference signal. It's crucial to note that this interference signal is characterized by a lower transmit power compared to the primary signal transmitted by the bladeRF device. This arrangement and the consequent angular relationships are designed to emulate and study certain real-world scenarios where a primary signal and interference coexist with varying power levels and angular orientations.

Figure 555 – Generating interference from Adalm-Pluto SDR device

Parameter	Value
Center frequency	1.5 GHz
Symbol rate	100 kHz
Tx Gain	-10 dB
Frequency of sinusoidal signal	12000
Sample rate of sinusoidal signal	100 kHz

Table 5 - Parameters of Adalm-Pluto Device

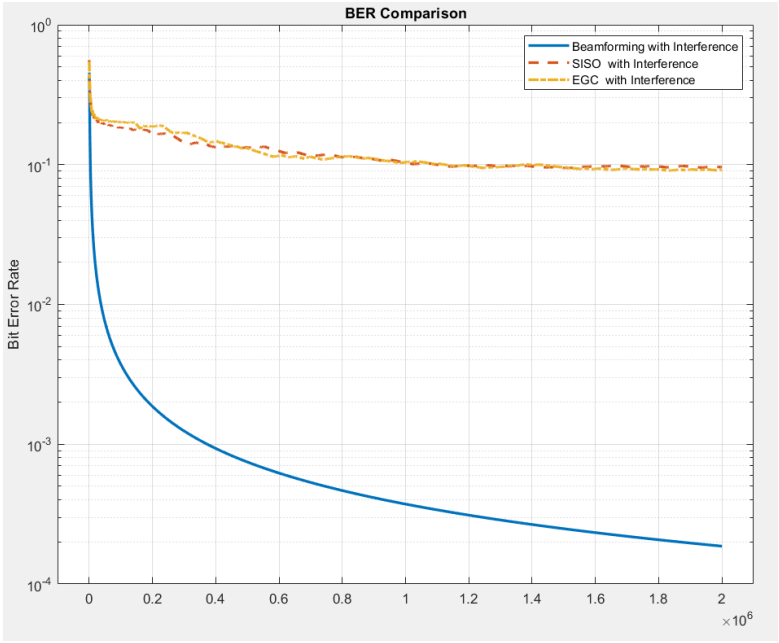

Figure 56 - BER Comparison of the systems with interference signal

From an analysis of Figure 56, the BER performance dynamics present a compelling narrative on the efficacy of different systems in environments fraught with interference. The 1x2 Beamforming system notably outshines both the 1x2 receive diversity employing EGC and the SISO system, especially in the presence of interference signals. The stark difference in performance underscores the inherent capability of beamforming to offer spatial selectivity. This spatial selectivity allows the beamforming system to focus its reception on the desired signal source while concurrently attenuating or nullifying the interference, effectively enhancing the Signal-to-Interference-plus-Noise Ratio (SINR). On the other hand, while the 1x2 receive diversity with EGC can harness multiple antennas to combat fading, it might not be as adept at negating the effects of directional interference. The traditional SISO configuration, with its lack of spatial processing capabilities, understandably struggles the most in this interference-rich scenario. In essence, Figure 54 vividly illustrates the superiority of the 1x2 beamforming technique in environments where interference signals are prevalent, demonstrating its marked advantage over both 1x2 receive diversity and SISO systems.

4.4.2.2. 2x1 Beamforming at Transmitter Side

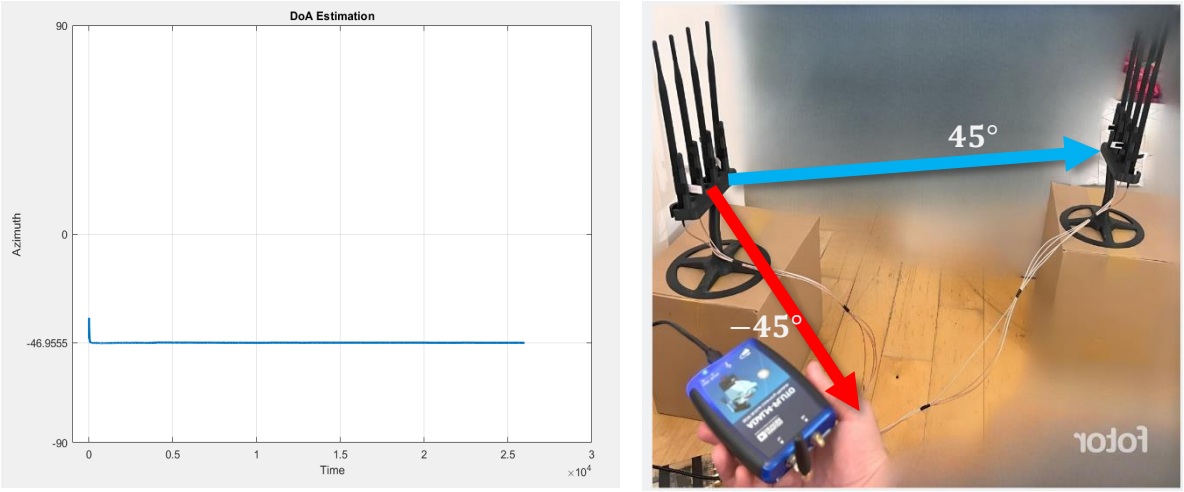

Figure 57 – Beam steering angle of transmitter in shown practical wireless communication system

Figure 57 shows the same setup in Figure 54, but in the meticulously arranged experimental setup, the transmitter's placement is of paramount importance. It's aligned in a manner that positions it at a 45-degree angle with respect to the bladeRF receiver device's antennas. Simultaneously, its orientation sets it at a contrasting -45-degree angle relative to the receiver antenna of the ADALM-Pluto device. This calculated positioning enables the transmitter's beam to be steered directly towards the bladeRF receiver, angled precisely at 45 degrees. The outcome of this precision-steering ensures that the beam's path is keenly focused and optimized for the bladeRF device. Given the directionality and exclusivity of this beam, the ADALM-Pluto receiver device, situated outside this transmission cone, is essentially left out of the communication link. As such, it remains untouched by the transmitted signal, reinforcing the idea that sharp beam steering can effectively manage and limit signal reception to targeted devices.

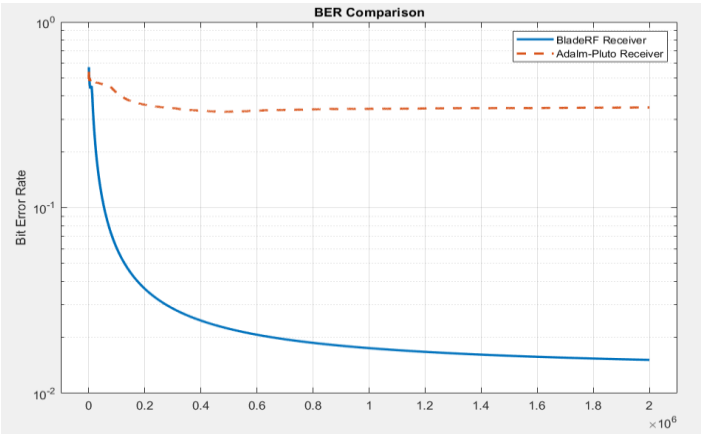

Figure 58 - BER Comparison of Adalm-Pluto receiver and BladeRF Receiver

Figure 58 clearly shows that Adalm-Pluto receiver cannot receive the transmitted signal from the 2x1 bladeRF transmitter while bladeRF receives the transmitted signal.

Chapter 5 : Conclusion

As we reflect upon this dissertation's journey, each chapter serves as a milestone highlighting the progression of understanding and application. Chapter 1 initiated our discourse, outlining the project's core description and primary objectives. Central to the endeavor was the development of practical digital wireless communication, subsequently enriched by the integration of digital beamforming using dual bladeRF SDR devices. Progressing to Chapter 2, a foundation was laid, providing crucial background knowledge essential for the comprehension of methodologies and techniques harnessed to attain our specified goals. Delving deeper in Chapter 3, we explored the intricate methods that underpin digital communication. This chapter spotlighted the utility of the MATLAB/Simulink environment, which was instrumental in crafting practical wireless communication while adeptly navigating its inherent challenges. Notably, a unique MIMO block was conceived and developed by the author, specifically tailored to facilitate MIMO communication with the bladeRF device. This innovation stands as a testament to the project's contributions, with aspirations that this block will serve as a valuable asset for the broader community. Transitioning to Chapter 4, the focus shifted to the empirical, as a suite of designed wireless communication systems - SISO QPSK, 1x2 Receive diversity with EGC algorithm, 1x2 Receiver beamforming, and 2x1 Transmitter beamforming - underwent rigorous testing and comparative analysis. An additional layer of complexity was introduced with the ADALM-Pluto SDR device, which was employed to generate interference, enabling an in-depth exploration into the BER characteristics of our primary wireless systems within such perturbed environments. Ultimately, the culmination of these endeavors led to a profound discussion, dissecting and deliberating upon the gathered results. This dissertation, in its entirety, represents not just an academic exercise but a deep dive into the practical realms of wireless communication, offering invaluable insights and tools for the field. In addition, all the files were used in this project are provided in Appendix C.

5.1. Future Work

This project has laid a solid foundation but also highlights avenues for further exploration and expansion. Due to current software constraints, the scope of our investigation was confined to the 1x2 and 2x1 antenna structures, limiting our ability to execute real-time programs directly on the host computer. However, the dynamic landscape of technology promises continued evolution. Future endeavors can capitalize on platforms equipped with enhanced computational capabilities tailored for real-time applications. Such advancements will not only facilitate the integration of a greater number of antennas but will also pave the way for the deployment of more sophisticated and contemporary algorithms. This, in turn, could usher in a new era of wireless communication systems that are more resilient, efficient, and adaptable to the ever-growing demands of the digital age. The potential for growth and refinement is substantial, and this project serves as an initial steppingstone towards that expansive horizon.

References

[1] A. F. Molisch, Wireless Communication, vol. 34, John Wiley & Sons, 2012, p. 4.

[2] M. S. John G. Proakis, Digital Communications, 5th ed., McGraw-Hill, Higher Education, 2008, p. 1.

[3] R. a. M. M. Roka, "Modeling Of the Psk Utilization At The Signal Transmission In The Optical Transmission Medium," *International Journal of Communication Networks and Information Security (Ijcnis),* vol. 3, no. 7, 2022.

[4] P. B. R. Durga Sowjanya Kolluru, "Review on communication technologies in telecommunications from conventional telephones to smart phones," *AIP Conference Proceedings,* vol. 2407, no. 1, 1 December 2021.

[5] R. K. Saha, "Coexistence of Cellular and IEEE 802.11 Technologies in Unlicensed Spectrum Bands -A Survey," *IEEE Open Journal of the Communications Society,* vol. 2, pp. 1996-2028, 2021.

[6] N. Dinh, "Proposal of Cooperative Communication to Enhance Accuracy of Wireless Control Systems," *Communications and Network,* vol. 11, pp. 52-63, 2019.

[7] A. A. A. M. A. M. M. A. A. M. Y. H. N. A. A. Aziz, "Physical Layer Security Using Scrambled BCH with Adaptive Granular HARQ," *Proceedings of the Multimedia University Engineering Conference (MECON 2022),* pp. 58-67, 2022.

[8] T. E. H. a. A. H. A. Nosratinia, "Cooperative communication in wireless networks," *IEEE Communications Magazine,* vol. 42, no. 10, pp. 74-80, October 2004.

[9] K. Wesolowski, Introduction to digital communication systems, John Wiley & Sons, 2009, pp. 3-6.

[10] F. Ouyang, Digital Communication for Practicing Engineers, John Wiley & Sons., 2019.

[11] S. S. a. M. M. Haykin, Modern wireless communications, Pearson Education India, 2005.

[12] D. K. A. M. a. R. S. Sharma, "Analog & digital modulation techniques: an overview," *International Journal of Computing Science and Communication Technologies 3,* vol. 3, no. 1, p. 2007, 2010.

[13] M. Miyake, "A survey on progress and standardization trends in wireless communications," *J. Commun.,* vol. 4, no. 7, pp. 509-520, 2009.

[14] L. Frenzel, "Understanding modern digital modulation techniques," *Electron. Des. Technol. Commun,* 2012.

[15] K. D. Wong, Fundamentals of wireless communication engineering technologies, vol. 98, John Wiley & Sons, 2011.

[16] Q. A. N. R. G. M. a. S. X. N. Mohammed El-Hajjar, "Demonstrating the Practical Challenges of Wireless Communications Using USRP," *IEEE Communications Magazine,* vol. 52, no. 5, pp. 194-201, 2014.

[17] Z. W. X. H. a. W. W. N. Zhang, "Digital automatic gain control design with large dynamic range in wireless communication receivers," *IEEE 17th International Conference on Communication Technology (ICCT),* pp. 1402-1406, 2017.

[18] F. Xiong, Digital modulation techniques, 2nd ed., London, 2006.

[19] P. J. Husted, "Design and Implementation of Digital Timing Recovery and Carrier Synchronization for High Speed Wireless Communication," 2000.

[20] A. F. V. V. R. S. H. Z. L. S. L. H. N. L. L. a. K. H. Molisch, "Hybrid beamforming for massive MIMO: A survey," *IEEE Communications magazine,* vol. 55, no. 9, pp. 134-141, 2017.

[21] R. W. N. G.-P. S. R. W. R. a. A. M. S. Heath, "An overview of signal processing techniques for millimeter wave MIMO systems," *IEEE journal of selected topics in signal processing,* vol. 10, no. 3, pp. 436-453, 2016.

[22] A. G. T. K. N. Bindle, "A detailed introduction of different beamforming techniques used in 5G," *International Journal of Communication Systems,* vol. 34, no. 5, 2021.

[23] E. M. I. R. N. a. N. F. A. Ali, "Beamforming techniques for massive MIMO systems in 5G: overview, classification, and trends for future research," *Frontiers of Information Technology & Electronic Engineering,* vol. 18, pp. 753-772, 2017.

[24] L. P. M. M. L. P. A. &. C. S. Rao, "5G beamforming techniques for the coverage of intended directions in modern wireless communication: In-depth review," *International Journal of Microwave and Wireless Technologies,* vol. 13, no. 10, pp. 1039-1062, 2021.

[25] J. X. Y. a. K. B. L. Zhang, "Hybrid beamforming for 5G and beyond millimeter-wave systems: A holistic view," *IEEE Open Journal of the Communications Society,* vol. 1, pp. 77-91, 2019.

[26] T. Ulversoy, "Software Defined Radio: Challenges and Opportunities," *IEEE Communications Surveys & Tutorials,* vol. 12, no. 4, pp. 531-550, 2010.

[27] B. D. Rami Akeela, "Software-defined Radios: Architecture, state-of-the-art, and challenges," *Computer Communications,* vol. 128, pp. 106-125, 2018.

[28] J. D. Gibson, Digital Communications: Introduction to Communication Systems, Springer Nature, 2023.

[29] "Adalm-Pluto Software-Defined Radio Active Learning Module," [Online]. Available: https://www.analog.com/en/design-center/evaluation-hardware-and-software/evaluation-boards-kits/adalm-pluto.html#eb-overview. [Accessed 2023 08 10].

[30] "HackRF," 12 Jun 2023. [Online]. Available: https://hackrf.readthedocs.io/_/downloads/en/latest/pdf/. [Accessed 2023 08 10].

[31] "RTL-SDR Blog V3 Datasheet," [Online]. Available: https://www.rtl-sdr.com/wp-content/uploads/2018/02/RTL-SDR-Blog-V3-Datasheet.pdf. [Accessed 15 08 2023].

[32] "bladeRF 2.0 micro xA4," [Online]. Available: https://www.nuand.com/product/bladerf-xa4/. [Accessed 2023 08 10].

[33] J. Szymaniak, "BLADERF WINDOWS®INSTALL GUIDE, INSTALLING BLADERF SOFTWARE WITH MATLAB®& SIMULINK®SUPPORT," Nuand, 2016.

[34] "QPSK Transmitter and Receiver in Simulink," [Online]. Available: https://uk.mathworks.com/help/comm/ug/qpsk-transmitter-and-receiver-in-simulink.html. [Accessed 1 06 2023].

[35] R. J. V. &. D. H. Mehra, “Scrambling of data in all-optical domain,” *Journal of Optics,* vol. 44, no. 3, pp. 220-224, 2015.

[36] D. a. L. Y. Shin, “Application Of Qim Based Audio Watermarking For Synchronizing Detection In the Air Environment,” *International Journal of Advanced Science and Technology,* vol. 112, pp. 57-66, 2018.

[37] A. R. a. S. A. B. Sherafat, “Comparison of Different Beamforming-Based Approaches for Sound Source Separation of Multiple Heavy Equipment at Construction Job Sites,” *2020 Winter Simulation Conference (WSC),* pp. 2435-2446, 2020.

[38] D. F. a. C. Z. D. E. Ba, “Enhanced MVDR Beamforming for Arrays of Directional Microphones,” *IEEE International Conference on Multimedia and Expo,* pp. 1307-1310, 2007.

[39] W. a. S. W. Liu, Wideband beamforming: concepts and techniques, John Wiley & Sons, 2010.

[40] “Tri-Band Antenna,” Nuand, [Online]. Available: https://www.nuand.com/product/tri-band-antenna/. [Accessed 06 06 2023].

[41] I. H. K. A. S. A. M. K. S. K. E. D. P. a. I. M. Ahmed, “A survey on hybrid beamforming techniques in 5G: Architecture and system model perspectives.,” *IEEE Communications Surveys & Tutorials,* vol. 20, no. 4, pp. 3060-3097, 2018.

[42] “USRP N210,” [Online]. Available: https://www.ettus.com/all-products/un210-kit/. [Accessed 10 08 2023].

Appendix A

https://drive.google.com/drive/folders/1iQx1yMWvjpoBvtlDTgvGSIAGc4qwz2J0?usp=sharing

Appendix B

https://drive.google.com/file/d/1W7So4PMUwuVPj99Bh8gSdbTlDv0ty6LW/view?usp=sharing

Appendix C

https://drive.google.com/drive/folders/1LAJJ-r2oeZ4vbJ4GWO_XXrpfhW2PaslG?usp=sharing